Journal of Medicinal Chemistry

Article

pubs.acs.org/jmc

Scaffold Diversity Inspired by the Natural Product Evodiamine: Discovery of Highly Potent and Multitargeting Antitumor Agents

Shengzheng Wang,[†,‡,∥] Kun Fang,[†,∥] Guoqiang Dong,[†,∥] Shuqiang Chen,[†] Na Liu,[†] Zhenyuan Miao,[†] Jianzhong Yao,[†] Jian Li,[§] Wannian Zhang,[†] and Chunquan Sheng*[,†]

[†]Department of Medicinal Chemistry, School of Pharmacy, Second Military Medical University, 325 Guohe Road, Shanghai 200433, People's Republic of China

[‡]School of Pharmacy, Fourth Military Medical University, 169 Changle West Road, Xi'an, 710032, People's Republic of China

[§]School of Pharmacy, East China University of Science & Technology, 130 Meilong Road, Shanghai 200237, People's Republic of China

Supporting Information

ABSTRACT: A critical question in natural product-based drug discovery is how to translate the product into drug-like molecules with optimal pharmacological properties. The generation of natural product-inspired scaffold diversity is an effective but challenging strategy to investigate the broader chemical space and identify promising drug leads. Extending our efforts to the natural product evodiamine, a diverse library containing 11 evodiamine-inspired novel scaffolds and their derivatives were designed and synthesized. Most of them showed good to excellent antitumor activity against various human cancer cell lines. In particular, 3-chloro-10-hydroxyl thio-evodiamine (**66c**) showed excellent *in vitro* and *in vivo* antitumor efficacy with good tolerability and low toxicity. Antitumor mechanism and target profiling studies indicate that compound **66c** is the first-in-class triple topoisomerase I/topoisomerase II/tubulin inhibitor. Overall, this study provided an effective strategy for natural product-based drug discovery.

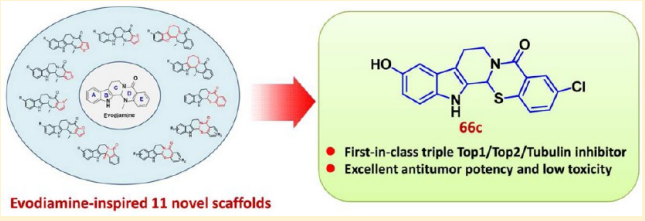

INTRODUCTION

Natural products (NPs) have been an important source of bioactive molecules for the development of therapeutic drugs.[1−3] NPs have evolved to target multiple proteins[4,5] and often possess diverse biological activities, which lead to a combination of therapeutic effects and toxicity.[5] The scaffolds of NPs can be regarded as "'bioactive'" or "privileged" scaffolds in chemical space because they have been naturally selected in evolution to specifically interact with a diversity of biological targets. However, the probability of developing an isolated NP directly into a therapeutic drug is relatively low. In most cases, NPs are used as biologically prevalidated starting points for drug discovery and development. Thus, a critical question to be answered is how to translate NPs into drug-like molecules with optimized pharmacological properties. The most commonly used method is the generation of large numbers of analogues by semisynthetic or total synthetic approaches. However, modifying NPs by simple derivatization or functional group transformations only achieved limited chemical diversity. Chemical space and structure−activity relationships (SARs) around NPs cannot be fully investigated. Scaffold diversity inspired by NPs allows for increased probability and quality to identify promising drug leads. To achieve this goal, several new strategies have been introduced, such as biology-oriented synthesis (BIOS),[4,6] diversity-oriented synthesis (DOS),[7,8] and diverted total synthesis (DTS).[9−11] Applications of these innovative methods indicated that the creation of NP-inspired scaffold diversity was proven to be a powerful tool to investigate new chemical space and identify novel lead compounds for drug discovery.[12−14]

Evodiamine (**1**, Figure 1) is a quinazolinocarboline alkaloid isolated from the fruit of *Evodia rutaecarpa* Bentham. Evodiamine has diverse biological activities including anti-inflammatory,[15−17] antiobesity,[18−21] and antitumor[22] effects. Among them, the antitumor activity of evodiamine has been extensively investigated. Evodiamine showed cytotoxicity against a variety of human cancer cell-lines by inducing apoptosis.[22,23] Moreover, it was a naturally multitargeting antitumor molecule, which exerted the antitumor activity by various molecular mechanisms such as

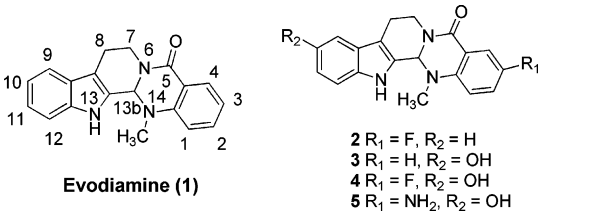

Figure 1. Chemical structures of evodiamine and its highly potent derivatives.

Received: June 14, 2015
Published: July 30, 2015

DOI: 10.1021/acs.jmedchem.5b00910
J. Med. Chem. 2015, 58, 6678−6696

Scheme 1[a]

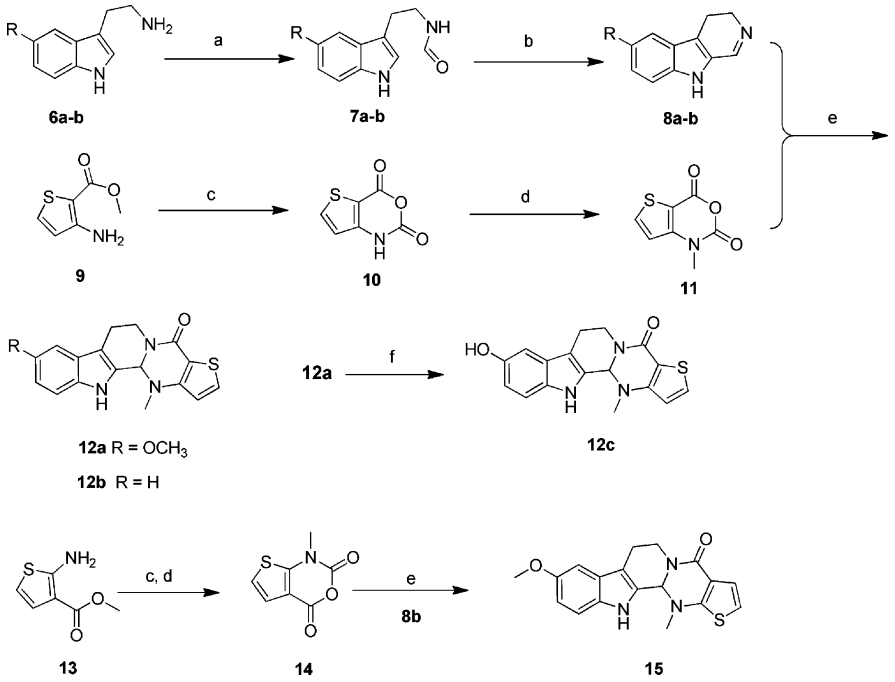

[a]Reagents and conditions: (a) ethyl formate, reflux, 6 h, yield 99%; (b) $POCl_3$, DCM, 0 °C, 6 h, yield 73−75%; (c) triphosgene, THF, reflux, 4 h; (d) CH_3I, KOH, DMF, 2 h, two step yield 52%; (e) CH_2Cl_2, rt, 3 h, yield 78−79%; (f) BBr_3, DCM, −78 °C, 2.5 h, yield 49%.

Scheme 2[a]

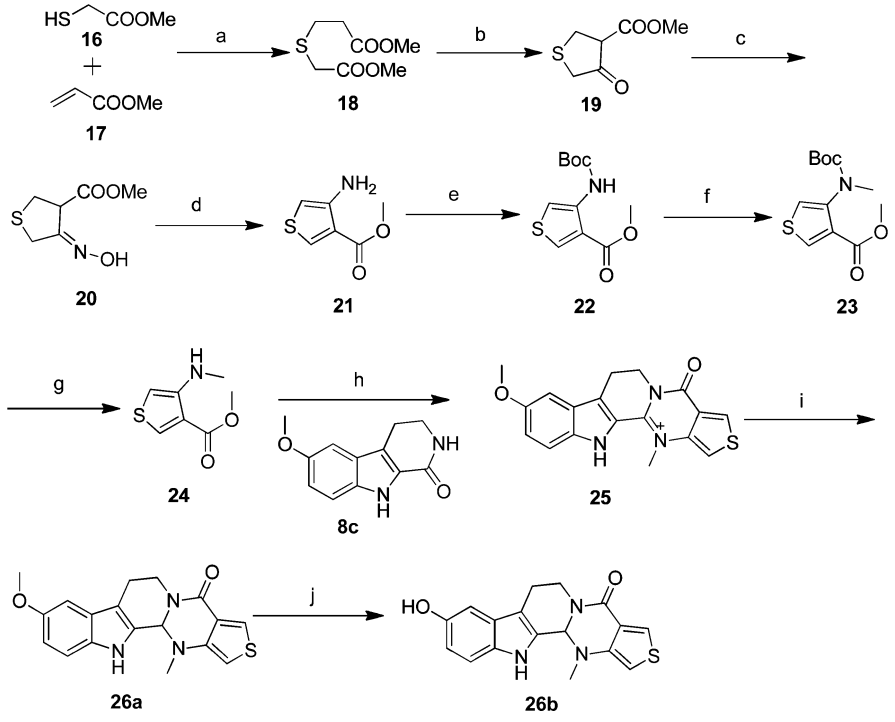

[a]Reagents and conditions: (a) piperidine, 50 °C, 2 h, yield 99%; (b) NaH, THF, reflux, 5 h, yield 35%; (c) NH_2OH, HCl, $BaCO_3$, MeOH, reflux, overnight, yield 98%; (d) HCl, ether-MeOH, rt, 24 h, yield 91%; (e) $(Boc)_2O$, DMAP, DCM, overnight, yield 40%; (f) MeI, NaH, DMF, 6 h, yield 84%; (g) CF_3COOH, CH_2Cl_2, rt, 2.5 h, yield 98%; (h) $POCl_3$, toluene, microwave, 130 °C,45 min; (i) $NaBH_4$, EtOH, rt, 1 h, two steps yield 27%; (j) BBr_3, DCM, −78 °C, 2.5 h, yield 43%.

caspase-dependent[24−28] and -independent[29] pathways, sphingomyelin pathway,[30] calcium/JNK signaling,[31] and PI3K/Akt/caspase and Fas-L/NF-κB signaling pathways.[32] Because of its broad-spectrum and multitargeting antitumor profile, evodiamine represents a good starting point for the development of novel antitumor agents.

Previously, we identified topoisomerase I (Top1) as one of the molecular targets of evodiamine by structure-based virtual

DOI: 10.1021/acs.jmedchem.5b00910
J. Med. Chem. 2015, 58, 6678−6696

Scheme 3[a]

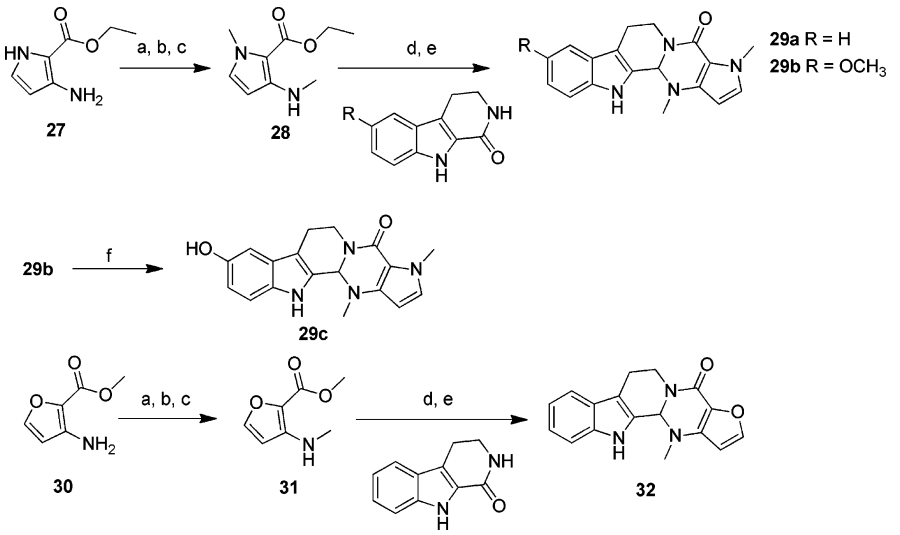

[a]Reagents and conditions: (a) $(Boc)_2O$, DMAP, CH_2Cl_2, overnight, yield 40−45%; (b) MeI, NaH, DMF, 6 h, yield 84−89%; (c) CF_3COOH, CH_2Cl_2, rt, 2.5 h, yield 94−97%; (d) $POCl_3$, toluene, microwave, 130 °C, 45 min; (e) $NaBH_4$, EtOH, rt, 1 h, yield 36−56% over two steps; (f) BBr_3, CH_2Cl_2, −78 °C, 2.5 h, yield 56%.

Scheme 4[a]

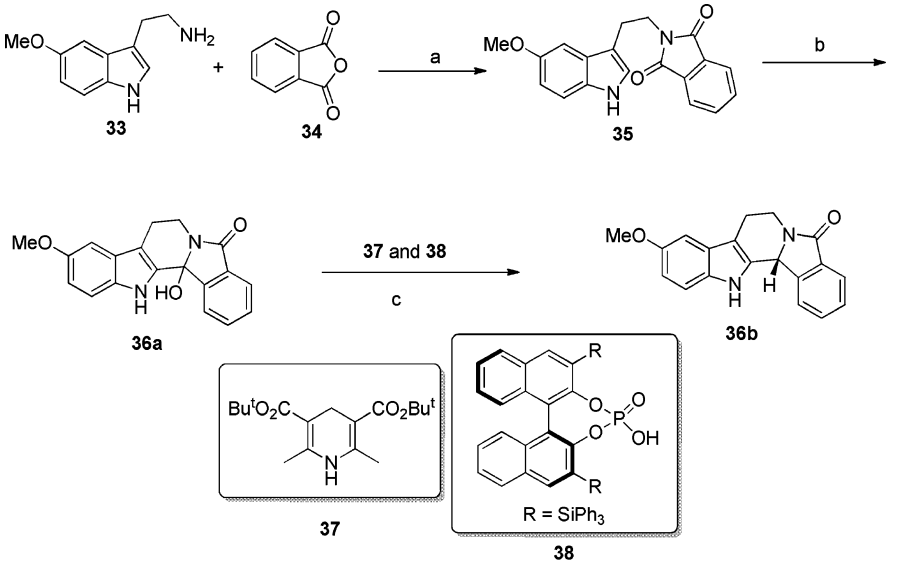

[a]Reagents and conditions: (a) toluene, reflux, 5 h; (b) TfOH, DCM, 0 °C, 30 min, yield 49% over two steps; (c) Hantzsch ester **37**, chiral phosphoric acid **38**, dioxane, rt, 3 h, yield 87%.

screening.[33] Subsequently, a number of substituted evodiamine derivatives were designed and synthesized.[34−36] Interestingly, several analogues, such as 3-fluoroevodiamine (**2**), 10-hydroxylevodiamine (**3**), 3-fluoro-10-hydroxylevodiamine (**4**), and 3-amino-10-hydroxylevodiamine (**5**), showed excellent antitumor activity at low nanomlar range.[34] Moreover, these evodiamine derivatives could significantly inhibit tumor growth in the A549 and HCT116 tumor xenograft models.[34] Interestingly, antitumor mechanism studies revealed that the evodiamine derivatives acted by dual inhibition of Top1 (poisons) and Top2 (catalytic inhibitors). The above work in combination with other reports[37−39] preliminarily clarified the SAR of substitutions on the evodiamine scaffold. In order to achieve an in-depth understanding of the chemical space around evodiamine, it is highly desirable to generate evodiamine-inspired scaffold diversity and investigate their biological activities.

CHEMISTRY

Chemical synthesis of evodiamine-inspired diverse scaffolds and their derivatives is depicted in Schemes 1−9. First, the E-ring phenyl group of evodiamine was replaced by various heterocycles including thiophene (**12a−c**, **15**, **26a−b**), pyrrole (**29a−c**), and furan (**32**). Among them, the synthesis of compounds **12a−c** and **15** was based on the coupling method similar to that in our previous report (Scheme 1).[33,34] Substituted 3,4-dihydro-*β*-carboline (intermediates **8a−b**) was prepared by reacting substituted tryptamine **6a−b** with ethyl formate and followed by intramolecular ring closure in the presence of $POCl_3$.[33] Intermediate **11** (or **14**) was prepared by reacting intermediate **9**

DOI: 10.1021/acs.jmedchem.5b00910
J. Med. Chem. 2015, 58, 6678−6696

Scheme 5[a]

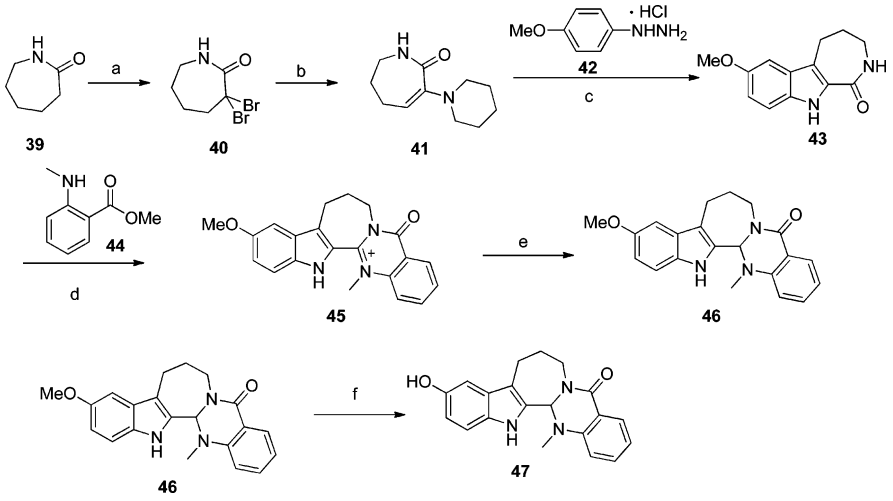

[a]Reagents and conditions: (a) PCl_5, ZnI_2, Br_2, N_2, $CHCl_3$, 0 °C, 6 h, yield 70%; (b) piperidine, N_2, reflux, 4.5 h, yield 91%; (c) EtOH, H_2SO_4, reflux, 5 h, yield 53%; (d) $POCl_3$, toluene, microwave, 130 °C, 45 min; (e) $NaBH_4$, EtOH, rt, 1 h, yield 38% over two steps; (f) BBr_3, CH_2Cl_2, −78 °C, 2.5 h, yield 46%.

Scheme 6[a]

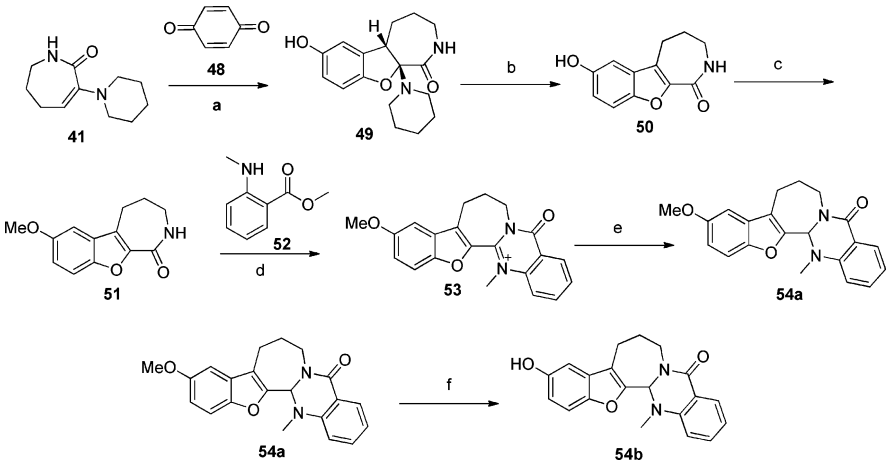

[a]Reagents and conditions: (a) acetone, 6 h, 20 °C, yield 47%; (b) AcOH, reflux, 4 h, yield 47%; (c) K_2CO_3, MeI, DMF, 4 h, yield 99%; (d) $POCl_3$, toluene, microwave, 130 °C, 45 min; (e) $NaBH_4$, EtOH, rt, 1 h, yield 65% over two steps; (f) BBr_3, CH_2Cl_2, −78 °C, 2.5 h, yield 56%.

(or **13**) with triphosgene, followed by methylation in the presence of CH_3I. Coupling of carbolines **8a−b** with intermediate **11** (or **14**) afforded compounds **12a−b** (or **15**). Hydroxyl substituted derivative **12c** was obtained by demethylation of compound **12a** in the presence of BBr_3 and DCM.

Starting from methyl 2-mercaptoacetate (**16**) and methyl acrylate (**17**), intermediate **24** was prepared via seven steps according to the reported methods.[40,41] Then, compound **26a** was prepared by reacting intermediate **24** and **8c** in the presence of $POCl_3$ under microwave conditions and followed by reduction in the presence of $NaBH_4$ (Scheme 2).[33] Using a similar protocol, scaffolds **29** and **32** were prepared (Scheme 3).

The synthetic method of compound **36b** was according to the procedure reported by You's group (Scheme 4).[42] First, 5-methoxyl-tryptamine (**33**) and phthalic anhydride (**34**) were refluxed in toluene to afford intermediate **35**. In the presence of TfOH, intramolecular cyclization of intermediate **35** afforded compound **36a**. Treatment of compound **35** with Hantzsch ester **37** and chiral phosphoric acid **38** in dioxane afforded compound **36b**. The absolute configuration of compound **36b** was in accordance with the literature data.[42]

Structural modification of the C-ring piperdine analogue of evodiamine was focused on ring expansion to the seven-membered ring and in combination with replacing AB-ring indole with benzofuran (compounds **46**, **47**, and **54a−b**). Starting from azepan-2-one (**39**), intermediate **43** was prepared via three steps according to the reported method.[43] In the presence of $POCl_3$, intermediates **43** and **44** were reacted under microwave conditions to afford quaternary ammonium salt **45**. After reduction by $NaBH_4$, compound **46** was obtained (Scheme 5). The synthesis of compound **54a** (Scheme 6) was similar to the synthetic method used for compound **46**. Hydroxyl substituted derivatives (**47** and **54b**) were obtained by demethylation of the corresponding methoxyl derivatives in the presence of BBr_3 and DCM.

The synthetic method for oxo-evodiamine derivatives is outlined in Schemes 7 and 8. First, substituted 2-hydroxy-benzoyl chloride (**56**) was prepared by reacting intermediate **55**

DOI: 10.1021/acs.jmedchem.5b00910
J. Med. Chem. 2015, 58, 6678−6696

Scheme 7[a]

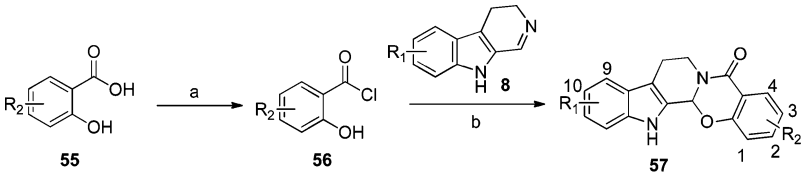

	R_1	R_2
57a	H	H
57b	H	1-OMe
57c	H	2-Cl
57d	H	2-Me
57e	H	2-CF_3
57f	H	2-OCH_3
57g	H	2-F
57h	H	3-OCH_3
57i	H	3-F
57j	H	3-Cl
57k	H	3-Br
57l	H	3-NO_2
57m	H	1,3-2Cl
57n	H	1,3-2I
57o	H	4-F
57p	H	4-CH_3

	R_1	R_2
57q	10-Cl	H
57r	10-OMe	H
57s	10-OMe	1-OCH_3
57t	10-OMe	2-Cl
57u	10-OMe	2-Me
57v	10-OMe	2-CF_3
57w	10-OMe	2-OCH_3
57x	10-OMe	2-F
57y	10-OMe	3-OCH_3
57z	10-OMe	3-F
57aa	10-OMe	3-Cl
57ab	10-OMe	3-Br
57ac	10-OMe	3-NO_2
57ad	10-OMe	1,3-2Cl
57ae	10-OMe	1,3-2I
57af	10-OMe	4-F
57ag	10-OMe	4-CH_3

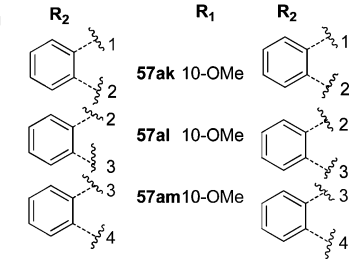

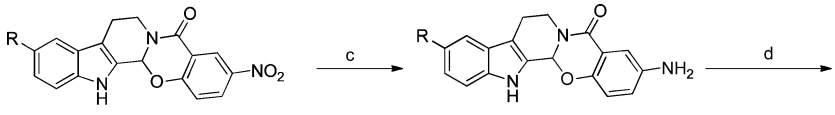

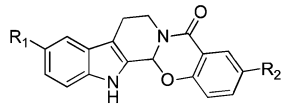

	R_1	R_2
57ap	H	3-NHCOCH$(CH_2)_2$
57aq	H	3-$NHCOCH_3$
57ar	H	3-$NHCH_2CH_3$
57as	H	3-$NHCH_2CH_2CH_3$
57at	H	3-$NHCH_2CH(CH_2)_2$
57au	H	3-$N(CH_2CH_2CH_3)_2$

[a]Reagents and conditions: (a) $SOCl_2$, DCM, reflux, 6 h, yield 98%; (b) intermediate **8**, DCM, rt, 6 h, yield 33%−56%; (c) H_2, Pd/C, EtOAc, yield 97%; (d) **57ap**−**57aq**, acyl chloride, Et_3N, DCM, yield 65%−73%; **57ar**−**57au**, aldehyde, $NaBH_3CN$, MeOH, yield 59%−82%.

Scheme 8[a]

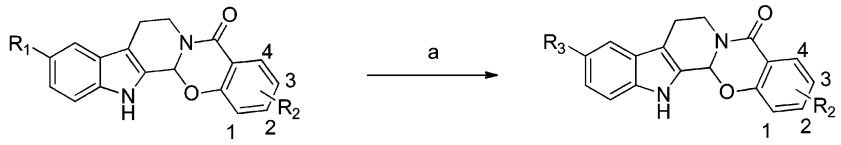

57

	R_3	R_2
58a	H	1-OH
55b	H	2-OH
58c	H	3-OH
58d	OH	H
58e	OH	1-OH
58f	OH	2-Cl
58g	OH	2-CH_3
58h	OH	2-CF_3

	R_3	R_2
58i	OH	3-OH
58j	OH	3-NH_2
58k	OH	3-Cl
58l	OH	3-Br
58m	OH	1,3-2Cl
58n	OH	4-CH_3

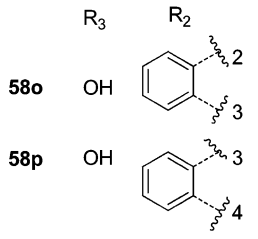

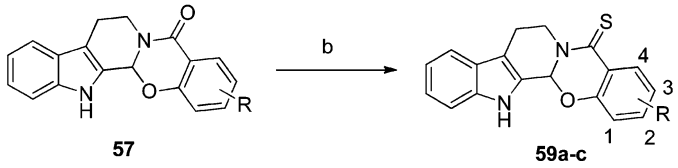

59a R = H
59b R = 2-CH_3
59c R = 4-CH_3

[a]Reagents and conditions: (a) BBr_3, DCM, −78 °C−0 °C, 6 h, yield 32%−68%; (b) Lawesson's reagent, PhMe, reflux, 6 h, yield 73%−80%.

DOI: 10.1021/acs.jmedchem.5b00910
J. Med. Chem. 2015, 58, 6678−6696

Scheme 9[a]

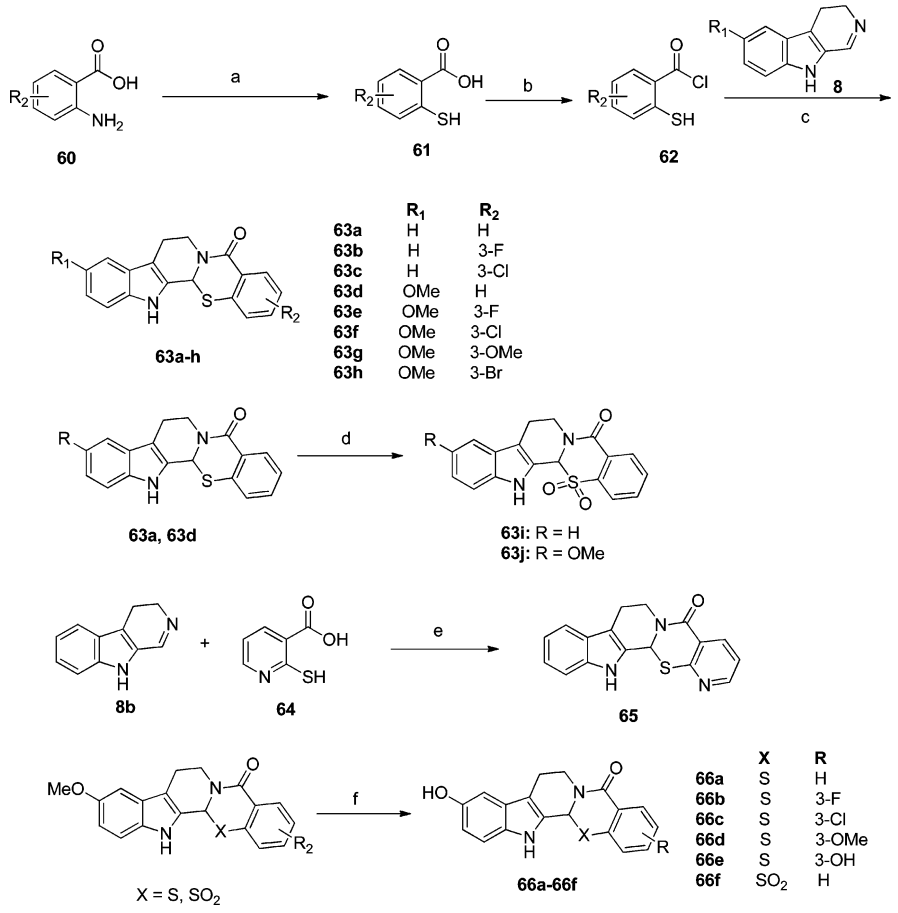

	R_1	R_2
63a	H	H
63b	H	3-F
63c	H	3-Cl
63d	OMe	H
63e	OMe	3-F
63f	OMe	3-Cl
63g	OMe	3-OMe
63h	OMe	3-Br

	X	R
66a	S	H
66b	S	3-F
66c	S	3-Cl
66d	S	3-OMe
66e	S	3-OH
66f	SO_2	H

[a]Reagents and conditions: (a) 1.1 $NaNO_2$, HCl, H_2O; 1.2 potassium ethylxanthate, H_2O, 80 °C/HCl (aq); 1.3 NaOH (aq), $Na_2S_2O_4$/HCl; (b) $SOCl_2$, DCM, reflux, 1 h; (c) DCM, rt, 6 h, yield 36%−55% over three steps; (d) H_2O_2, Na_2WO_4, AcOH, 55°C, 3 h, yield 63%−78%; (e) microwave, 120 °C, 30 min, yield 30%; (f) BBr_3, DCM, −78 °C−0°C, 6 h, yield 40%−70%.

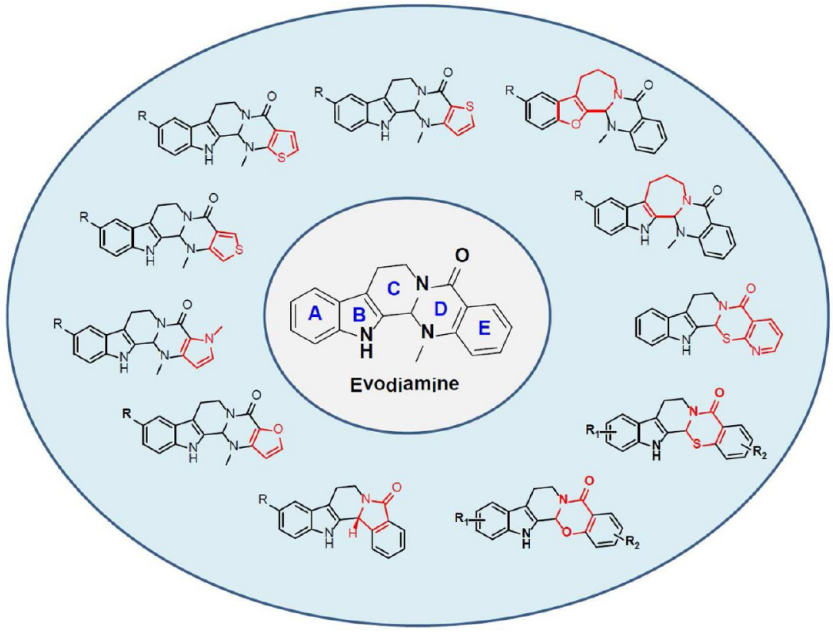

Figure 2. Evodiamine inspired scaffold diversity.

with $SOCl_2$ in DCM. Then, intermediate **56** and substituted 3,4-dihydro-β-carboline (**8**) were reacted at room temperature to afford derivatives **57**. Reduction of the nitro group of compounds **57l** and **57ac** using 10% Pd/C and H_2 afforded the amino

DOI: 10.1021/acs.jmedchem.5b00910
J. Med. Chem. 2015, 58, 6678−6696

derivatives **57an** and **57ao**. Compounds **57ap**−**57au** were synthesized by acylation or reductive amination of compounds **57an** and **57ao**. In the presence of BBr_3 and DCM, hydroxyl substituted derivatives (**58a**−**58p**) were prepared by demethylation of the corresponding methoxyl derivatives. Treatment of compounds **57** with Lawesson's reagent afforded thiocarboyl derivatives **59a**−**59c**.

The chemical synthesis of thio-evodiamine derivatives (**63a**−**66f**) is outlined in Scheme 9. Starting from substituted 2-aminobenzoic acids (**60**), various 2-mercapto-benzoic acids (**61**) were prepared according to reported protocols.[44] Then, intermediate **61** and $SOCl_2$ were refluxed in DCM for 1 h to obtain various 2-mercapto-benzoyl chlorides (**62**). Derivatives **63a**−**63h** were obtained by reacting intermediate **62** and substituted 3,4-dihydro-*β*-carboline (**8**) at room temperature. In the presence of H_2O_2 and Na_2WO_4, the sulfur atom of compounds **63a** and **63d** was oxidized to the sulfone (**63i** and **63j**). Under microwave conditions, intermediates **64** (commercial available) and **8b** were irradiated at 120 °C for 30 min to obtain compound **65**. Hydroxyl substituted derivatives (**66a**−**66f**) were obtained by demethylation of the corresponding methoxyl derivatives in the presence of BBr_3 and DCM.

RESULTS AND DISCUSSION

Evodiamine-Inspired New Scaffold Design. A series of evodiamine-inspired new scaffolds were designed according to chemical diversity and synthetic possibility (Figure 2). First, the E-ring phenyl of evodiamine was replaced by various heterocycles including thiophene, pyrrole, and furan. Second, the D-ring 2,3-dihydropyrimidin-4(1*H*)-one scaffold was converted into a five-membered 1*H*-pyrrol-2(5*H*)-one ring. Moreover, replacing D-ring *N*-methyl with oxygen or sulfur afforded oxo-evodiamine and thio-evodiamine. Third, the C-ring piperdine was enlarged to a seven-membered ring in combination with replacing AB-ring indole with benzofuran. As a result, 11 totally new scaffolds were designed and synthesized. Considering that the 10-hydroxyl group was important for improving the antitumor activity of evodiamine,[34] a 10-hydroxyl or 10-methoxyl group was introduced on the new scaffolds to investigate the difference of SARs between various scaffolds.

***In Vitro* Antitumor Activity of Evodiamine-Inspired New Scaffolds.** The evodiamine-inspired new scaffolds were assayed for growth inhibitory activities toward human cancer cell-lines A549 (lung cancer), MDA-MB-435 (breast cancer), and HCT116 (colon cancer) using the MTT assay.[33] Evodiamine and camptithecin were used as reference drugs. As shown in Table 1, several new scaffolds (e.g., **26b**, **54a**, **57a**, **64a**, and **66a**) showed good to excellent antitumor activity with a broad spectrum. The E-ring thiophene scaffold **12b** only showed weak antitumor activity. Introduction of a methoxyl group on the A-ring (compound **12a**) led to the loss of antitumor activity. After the demethylation of **12a**, the hydroxyl derivative **12c** showed improved antitumor activity toward the A549 (IC_{50} = 15.8 *μ*M) and HCT116 (IC_{50} = 23.6 *μ*M) cell lines. These SARs were similar to that of evodiamine.[34] Furthermore, movement of the sulfur atom in the thiophene ring (**15**, **26a**, and **26b**) resulted in the increase of the antitumor activity. Compound **26b** showed good activity against A549 (IC_{50} = 3.9 *μ*M), HCT116 (IC_{50} = 4.8 *μ*M), and MDA-MB-435 (IC_{50} = 32.3 *μ*M) cell lines. The pyrrole scaffold (**29a**−**c**) also showed broad-spectrum antitumor activity with a SAR similar to that of evodiamine, but they were less active than the thiophene scaffold **26b**. In contrast, the furan scaffold **32** was only weakly active. Similarly, the D-ring modified scaffolds

Table 1. *In Vitro* Antitumor Activity of Evodiamine-Inspired Scaffolds (IC_{50}, *μ*M)

compds	A549	HCT116	MDA-MB-435
12a	> 200	> 200	> 200
12b	110.7 ± 13.2	192.5 ± 15.7	> 200
12c	15.8 ± 1.1	23.6 ± 2.0	> 200
15	26.9 ± 3.1	14.1 ± 1.6	36.2 ± 2.5
26a	32.3 ± 2.7	94.9 ± 8.9	49.0 ± 4.3
26b	3.9 ± 0.20	4.8 ± 0.62	32.3 ± 2.9
29a	> 200	76.5 ± 6.2	206.7 ± 19.8
29b	28.5 ± 3.0	54.1 ± 5.1	42.0 ± 5.3
29c	5.0 ± 0.11	15.4 ± 2.0	11.7 ± 0.91
32	> 200	177.8 ± 1.8	181.6 ± 19.4
36a	> 200	> 200	> 200
36b	193.1 ± 18.2	30.9 ± 3.5	> 200
46	> 200	> 200	> 200
47	32.4 ± 3.3	59.8 ± 6.4	69.2 ± 5.9
54a	6.2 ± 0.41	5.3 ± 0.55	28.4 ± 3.1
54b	> 200	> 200	> 200
57a	2.4 ± 0.22	3.1 ± 0.28	3.0 ± 0.23
57r	> 200	> 200	> 200
58d	4.0 ± 0.31	2.3 ± 0.19	1.4 ± 0.20
64a	0.37 ± 0.01	0.52 ± 0.04	0.23 ± 0.03
64d	50.1 ± 5.2	0.5 ± 0.03	17.8 ± 1.5
66a	0.05 ± 0.004	0.04 ± 0.05	< 0.003
evodiamine	> 200	> 200	22.1 ± 2.3
CPT	0.10 ± 0.001	0.09 ± 0.005	1.00 ± 0.06

36a and **36b** also showed poor antitumor activity. When the C-ring of evodiamine was enlarged to a seven-membered ring, methoxyl derivative **46** was totally inactive, and the correspondingly hydroxyl derivative **47** showed moderate antitumor activity (IC_{50} range: 32.4 *μ*M−69.2 *μ*M). Interestingly, further changing the indole substructure of **46** to benzofuran (compound **54a**) led to significant increase of the antitumor activity (IC_{50} range: 5.3 *μ*M to 28.4 *μ*M). However, demethylation of compound **54a** yielded an inactive hydroxyl derivative **54b**, whose SAR was different from that of other scaffolds. The results indicated that the antitumor mechanism might be changed after scaffold morphing. Among the evodiamine-inspired scaffolds, oxo- and thio-evodiamine showed the best antitumor activity. The unsubstituted oxo-evodiamine (IC_{50} range: 1.4 *μ*M to 4.0 *μ*M) and thio-evodiamine (IC_{50} range: 0.23 *μ*M−0.52 *μ*M) were far more potent than the original evodiamine scaffold. Introduction of the 10-methoxyl group led to a decrease of the antitumor activity. For the corresponding hydroxyl derivatives, 10-hydroxyl-oxo-evodiamine (**58d**) showed activity similar to that of its original template. In contrast, 10-hydroxyl-thio-evodiamine (**66a**) was highly active with IC_{50} values against the A549, HCT116, and MDA-MB-435 cell lines of 0.05 *μ*M, 0.04 *μ*M, and <0.003 *μ*M, respectively, which was comparable or superior to camptothecin (CPT). Because of the excellent antitumor activity of oxo- and thio-evodiamine scaffolds, they were subjected to further SAR investigations.

SAR of the Oxo-evodiamine Derivatives. On the basis of the scaffold of oxo-evodiamine, a number of derivatives were designed and synthesized (Table 2). First, various substitutions were introduced on the E-ring (**57b**−**p**). The 1-methoxyl derivative (**57b**) showed better activity against the MDA-MB-435 cell line (IC_{50} = 2.21 *μ*M) than the original scaffold **57a** (IC_{50} = 3.0 *μ*M), but it was less active for the other two cancer cell lines. Moving the methoxyl group to positions 2 (**57f**) and 3 (**57h**) all

DOI: 10.1021/acs.jmedchem.5b00910
J. Med. Chem. 2015, 58, 6678−6696

Table 2. *In Vitro* Antitumor Activity of the Oxo-evodiamine Derivatives (IC_{50}, μM)

compds	A549	MDA-MB-435	HCT116	compds	A549	MDA-MB-435	HCT116
57b	26.8 ± 2.5	2.21 ± 0.21	16.90 ± 1.7	**58aj**	19.1 ± 2.3	21.6 ± 3.2	21.6 ± 2.3
57c	58.6 ± 5.3	40.6 ± 4.1	34.17 ± 3.3	**57ak**	>200	>200	>200
57d	62.5 ± 6.3	25.5 ± 1.7	97.23 ± 9.2	**57al**	>200	58.0 ± 5.7	34.8 ± 3.3
57e	25.8 ± 2.5	23.3 ± 2.2	21.87 ± 1.9	**57am**	>200	>200	31.00 ± 4.0
57f	174.2 ± 16.1	71.2 ± 7.5	52.34 ± 5.6	**57an**	2.7 ± 0.22	2.3 ± 0.21	9.1 ± 0.88
57g	95.0 ± 8.8	6.7 ± 0.57	170.81 ± 23.1	**57ao**	113.7 ± 10.9	42.8 ± 3.8	132.4 ± 12.8
57h	14.8 ± 2.3	25.6 ± 2.3	>200	**57ap**	28.4 ± 2.5	9.4 ± 6.9	11.7 ± 1.7
57i	6.6 ± 0.46	5.8 ± 0.61	46.10 ± 4.2	**57aq**	20.1 ± 1.8	5.8 ± 0.62	19.6 ± 2.3
57j	0.05 ± 0.002	1.4 ± 0.09	0.6 ± 0.05	**57ar**	>200	39.4 ± 3.7	>200
57k	1.6 ± 0.07	13.8 ± 1.2	3.7 ± 0.39	**57as**	173.2 ± 14.9	16.7 ± 1.9	>200
57l	>200	>200	>200	**57at**	>200	5.3 ± 5.1	>200
57m	1.8 ± 0.11	6.7 ± 0.66	14.2 ± 1.3	**57au**	>200	2.3 ± 0.21	>200
57n	>200	24.4 ± 2.1	>200	**58a**	103.3 ± 10.7	>200	42.3 ± 4.8
57o	35.1 ± 2.8	31.0 ± 3.6	71.0 ± 7.8	**58b**	17.5 ± 1.6	54.1 ± 4.5	29.3 ± 2.7
57p	>200	38.1 ± 0.32	>200	**58c**	16.2 ± 1.2	1.9 ± 0.23	11.5 ± 1.2
57q	3.49 ± 0.29	2.1 ± 0.19	5.59 ± 0.44	**58e**	>200	53.4 ± 5.0	66.2 ± 5.9
57s	>200	52.7 ± 5.6	80.1 ± 8.3	**58f**	10.6 ± 0.98	18.7 ± 1.6	7.1 ± 0.58
57t	3.8 ± 0.33	8.7 ± 0.79	4.6 ± 0.48	**58g**	6.5 ± 0.54	<0.003	<0.003
57u	>200	>200	198.0 ± 18.7	**58h**	14.7 ± 1.2	10.9 ± 1.8	10.5 ± 1.1
57v	50.5 ± 4.7	31.7 ± 32.6	26.2 ± 2.3	**58i**	3.8 ± 0.32	1.2 ± 0.14	0.8 ± 0.08
57w	>200	>200	>200	**58j**	29.1 ± 2.1	0.5 ± 0.06	0.6 ± 0.03
57x	>200	37.1 ± 3.6	156.7 ± 13.1	**58k**	5.2 ± 0.44	< 0.003	0.06 ± 0.004
57y	9.5 ± 0.85	23.7 ± 1.9	10.1 ± 1.0	**58l**	0.06 ± 0.005	<0.003	<0.003
57z	13.1 ± 1.2	25.1 ± 2.3	36.4 ± 3.2	**58m**	8.6 ± 0.72	7.0 ± 0.84	0.3 ± 0.02
57aa	0.05 ± 0.003	1.0 ± 0.11	2.4 ± 0.19	**58n**	1.8 ± 0.09	<0.003	<0.003
57ab	2.6 ± 0.1	5.4 ± 0.48	7.1 ± 0.77	**58o**	5.6 ± 0.43	5.1 ± 0.47	5.1 ± 0.47
57ac	>200	>200	>200	**58p**	3.1 ± 0.26	6.3 ± 0.61	2.7 ± 0.30
58ad	7.7 ± 0.68	13.9 ± 1.4	21.0 ± 1.3	**59a**	7.7 ± 0.69	5.6 ± 0.48	4.8 ± 0.39
58ae	>200	182.3 ± 17.5	>200	**59b**	65.2 ± 8.0	44.4 ± 4.8	60.3 ± 5.8
58af	>200	145.00 ± 13.9	>200	**59c**	11.0 ± 1.6	3.8 ± 0.35	4.5 ± 0.41
58ag	10.9 ± 1.3	3.5 ± 0.26	18.4 ± 1.6	CPT	0.7 ± 0.06	<0.003	0.02 ± 0.001
58ah	>200	176.1 ± 10.2	169.0 ± 17.3	TPT	7.4 ± 0.82	0.7 ± 0.09	0.4 ± 0.03
58ai	187.9 ± 17.6	>200	>200	IRT	20.1 ± 2.8	18.6 ± 1.2	6.3 ± 0.77

led to decreased activity. All of the 2-substituted (**57c−g**) and 4-substituted (**57o−p**) derivatives only showed moderate antitumor activity. In contrast, the 3-chloro analogue **57j** showed good activity particularly for the A549 cell line (IC_{50} = 0.05 μM). The 3-fluoro (**57i**), 3-bromo (**57k**), and 1,3-disubstituted (**57m−n**) derivatives were less potent, whereas the 3-nitro derivative **57l** was totally inactive. When the nitro group of **57l** was reduced to the amine, compound **57an** showed good antitumor activity (IC_{50} range: 2.7 μM−9.1 μM). However, further substitution or acylation of **57an** led to the decrease of the activity (**57ap−au**). However, annulation the E-ring with phenyl at different positions (**57ah−am**) was also unfavorable for the activity.

Second, the carbonyl group of oxo-evodiamine (**57a**) was converted into thiocarbonyl group (**59a−c**). However, these thiocarbonyl derivatives generally showed decreased antitumor activity. Third, a series of 10-hydroxyl (**58a−p**) as well as 10-methoxyl (**57s−57ag**) oxo-evodiamine derivatives were synthesized. In general, the methoxyl derivatives only showed moderate antitumor activity with the exception of compound **57aa**. The 3-chloro-10-methoxyl analogue **57aa** was highly active against the A549 cell line (IC_{50} = 0.05 μM), which was much better than all the reference drugs including CPT, topotecan (TPT), and irinotecan (IRT). Notably, the 3-chloro derivative **57j** also showed excellent antitumor activity, indicating that the 3-chloro substitution was important for activity.

Interestingly, significant improvement of the antitumor activity was observed for the hydroxyl derivatives. Moreover, the hydroxyl group was more favorable at the A-ring than the E-ring. For example, 1-hydroxyl (**58a**), 2-hydroxyl (**58b**), and 3-hydroxyl (**58c**) derivatives were moderately active. In contrast, most of the 10-hydroxyl derivatives showed significantly better activity. Particularly, compounds **58g**, **58k**, **58l**, and **58n** were the most active oxo-evodiamine derivatives. The IC_{50} value of compounds **58g**, **58k**, **58l**, and **58n** against the MDA-MB-435 cell line was lower than 3 nM, which was comparable to that of CPT and superior to those of TPT and IRT. For the HCT116 cell line, compounds **58g**, **58l**, and **58n** were far more potent than the reference drugs with an IC_{50} value of lower than 3 nM. SAR analysis revealed that the 1,10-dihydroxyl substitution (**58e**) was unfavorable and that 3,10-dihydroxyl substitution (**58i**) resulted in a slight increase of activity. On the basis of 10-hydroxyl oxo-evodiamine (**58d**), further introduction of 2-methyl (**58g**), 3-amino (**58j**), 3-chloro (**58k**), 3-bromo (**58l**), and 4-methyl (**58n**) led to substantial improvement of the antitumor activity, whereas further annulations of the E-ring phenyl group (**58o−p**) had little effect.

SAR of the Thio-evodiamine Derivatives. Because of the promising antitumor profile of thio-evodiamine (**63a**) and 10-hydroxyl-thio-evodiamine (**66a**), a series of substituted derivatives were investigated. As shown in Table 3, the introduction of 3-fluoro (**63b**) and 3-chloro (**63c**) substituents on compound

DOI: 10.1021/acs.jmedchem.5b00910
J. Med. Chem. 2015, 58, 6678−6696

Table 3. *In Vitro* Antitumor Activity of the Thio-evodiamine Derivatives (IC_{50}, μM)

compds	A549	MDA-MB-435	HCT116
63b	>200	>200	>200
63c	2.1 ± 0.12	29.1 ± 2.6	38.8 ± 3.9
63e	1.2 ± 0.10	6.5 ± 0.55	3.9 ± 0.29
63f	2.3 ± 1.9	2.7 ± 0.31	44.1 ± 5.0
63g	11.3 ± 1.0	20.0 ± 2.1	122.0 ± 13.7
63h	8.2 ± 0.79	2.7 ± 0.32	84.7 ± 8.8
63i	>200	>200	>200
63j	>200	>200	>200
65	>200	>200	>200
66b	1.2 ± 0.11	<0.003	<0.003
66c	0.02 ± 0.001	<0.003	<0.003
66d	0.3 ± 0.02	<0.003	<0.003
66e	0.7 ± 0.08	<0.003	<0.003
66f	>200	46.0 ± 4.3	>200
evodiamine	>200	>200	22.12 ± 1.9
CPT	0.7 ± 0.06	<0.003	0.02 ± 0.003
TPT	7.4 ± 0.69	0.7 ± 0.05	0.4 ± 0.02
IRT	20.1 ± 2.7	18.6 ± 1.7	6.3 ± 5.6

63a was unfavorable for antitumor activity. Moreover, all of the 3-substituted-10-methoxyl analogues (**63e−h**) showed moderate antitumor activity. Notably, after demethylation, the corresponding 10-hydroxyl derivatives (**66b−e**) were highly active at low nanomolar range. The IC_{50} values of compounds **66b−e** against HCT116 and MDA-MB-435 cell lines were lower than 3 nM. In particular, the 3-chloro-10-hydroxyl derivative **66c** revealed excellent inhibitory activity against all of the three cancer cell lines (IC_{50} range: 0.02 μM to <0.003 μM), highlighting its promising feature as a novel antitumor candidate. Further modification was focused on oxidation of the sulfur atom to sulfone (**63i**, **63j**, and **66f**). Unfortunately, these sulfone derivatives were almost inactive. Moreover, replacement of the phenyl group with pyridinyl (**65**) also led to a loss of activity.

Antitumor Spectrum of the Selected Oxo- and Thio-evodiamine Derivatives. An *in vitro* antitumor assay revealed that a number of oxo- and thio-evodiamine derivatives showed highly potent activity against the A549, HCT116, and MDA-MB-435 cell lines. To further evaluate their antitumor spectrum, several compounds (**58i**, **58k**, **66c**, **66d**, and **66e**) were tested against a variety of human cancer cell lines including SW579 (thyroid cancer), SK-Hep-1 (liver cancer), PC-3 (pancreatic cancer), NCI-H446 (small cell lung cancer), MV3 (melanoma cells), K562 (leukemia cells), and BEL7404 (liver cancer). As depicted in Table 4, all of the compounds showed good to excellent antitumor activity against the tested cancer cell lines with the exception of the NCI-H446 cell line. They were particularly effective against the K562 and BEL7404 cell lines with IC_{50} values lower than 3 nM, which were more potent than the positive control CPT. Among them, compound **66e** showed the best antitumor activity. It was highly active against the PC-3, K562, and BEL7404 cell lines with IC_{50} values lower than 3 nM. Moreover, it was also active against SK-Hep-1 and MV3 cell lines with IC_{50} values of 0.49 μM and 0.14 μM, respectively. These results confirmed that oxo- and thio-evodiamine derivatives had a broad antitumor spectrum, particularly for PC-3, K562, and BEL7404 cell lines, which were superior or comparable to that of CPT.

Effect of Selected Evodiamine Derivatives on Apoptosis and Cell Cycle Distribution in A549 Cells. To test the effect of novel oxo- and thio-evodiamine derivatives on the induction of apoptosis, compounds **58k** and **66a** were evaluated by cell morphology and fluorescene-activated cell sorting (Figure 3). After treating with 5 μM of compounds **58k** or **66a** for 36 h, the majority of A549 cells became small, round, and floating. In contrast, a normal shape and well-ordered cytoskeleton was observed in the untreated control group and DMSO group. After treating with compounds **58k** or **66a**, the percentage of apoptotic cells was 6.7% and 6.0%, respectively. In contrast, the percentage of apoptotic cells in the control and DMSO groups was 0.7% and 0.5%, respectively. These results indicated that oxo- and thio-evodiamine derivatives could effectively induce the cell morphology change of A549 cells and the apoptosis of cancer cells.

Evodiamine was reported to arrest PC-3 cells at the G_2/M phase.[45] Herein, the effect of oxo- and thio-evodiamines **58k** and **66a** on cell cycle progression of A549 cells was evaluated by the flow cytometric method (Figure 4 and Figure S1). The results showed that G_2/M arrest was initiated after a 12 h exposure to compounds **58k** and **66a**. After treating with compounds **58k** and **66a** at 5 μM for 36 h, the ratios in the G_2/M phase of the cell cycle were 63.7% and 68.2%, respectively. In contrast, the ratios of cells untreated or treated with DMSO in the G_2/M phase of the cell cycle were 11.9% and 8.0%, respectively. Thus, the two compounds could significantly arrest the A549 cell cycle at the G_2/M phase.

Top1 Inhibitory Activity and the Binding Modes. Previously, Top1 was found to be one of the antitumor targets of evodiamine derivatives.[33,34] They act by stabilizing a covalent Top1-DNA complex called the cleavable complex. To further evaluate the inhibitory effect of oxo- and thio-evodiamine derivatives on Top1-mediated DNA cleavage, representative compounds (i.e., compounds **58d**, **58i**, **58j**, **58k**, **63a**, **63j**, **66a**, **66c**, **66d**, and **66e**) were assayed. As shown in Figure 5, all of the tested compounds showed potent inhibitory activity against Top1-mediated relaxation of supercoiled DNA at a concentration of 200 μM. At a concentration of 100 μM, most thio-evodiamine derivatives (compounds **63a−66e**) retained potent inhibitory activity, but the oxo-evodiamine derivatives showed decreased activity (see Table S1 for inhibition rate). Moreover, good Top1 inhibitory activity was still observed for the thio-evodiamine derivatives at a concentration of 50 μM. The above

Table 4. *In Vitro* Antitumor Spectrum of the Selected Evodiamine Derivatives (IC_{50}, μM)

compds	SW579	SK-Hep-1	PC-3	NCI-H446	MV3	K562	BEL7404
58i	5.15 ± 0.48	1.1 ± 0.09	0.84 ± 0.07	>200	1.2 ± 0.09	<0.003	0.06
58k	5.56 ± 0.51	1.8 ± 0.11	0.40 ± 0.03	>200	1.1 ± 0.13	<0.003	<0.003
66c	6.9 ± 0.59	2.1 ± 0.19	0.37 ± 0.02	>200	1.3 ± 0.11	<0.003	<0.003
66d	7.3 ± 0.63	2.2 ± 0.13	0.43 ± 0.03	>200	1.2 ± 0.08	<0.003	<0.003
66e	3.5 ± 0.23	0.49 ± 0.03	<0.003	16.6 ± 1.4	0.14 ± 0.01	<0.003	<0.003
CPT	0.71 ± 0.69	0.96 ± 0.78	2.5 ± 0.12	>200	<0.003	<0.003	0.14 ± 0.01

DOI: 10.1021/acs.jmedchem.5b00910
J. Med. Chem. 2015, 58, 6678−6696

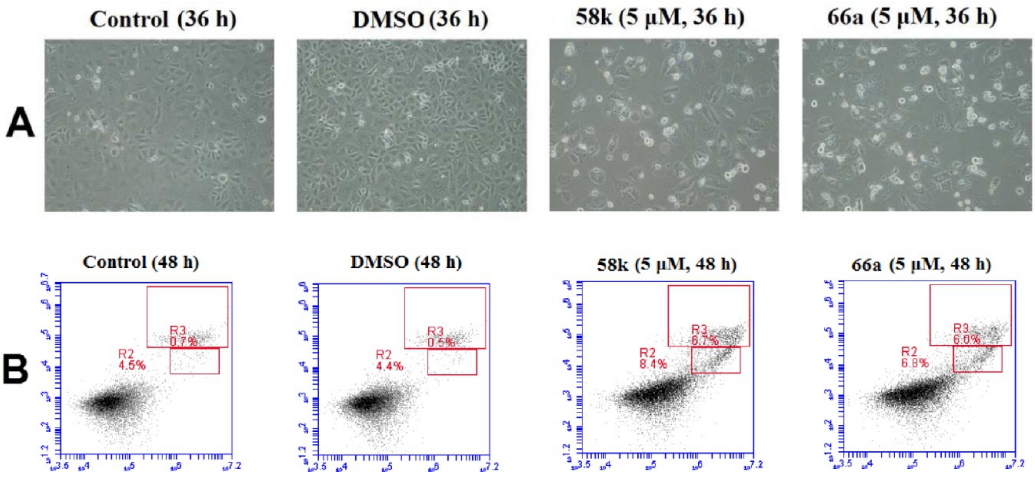

Figure 3. (A) Effect of evodiamine derivatives on human cancer cell morphology. A549 cells were treated with DMSO or 5 μM compounds **58k** or **66a** for 36 h, and representative photographs were captured under a light microscope. (B) Evodiamine derivatives-induced cell apoptosis. A549 cells were treated with DMSO or 5 μM of compounds **58k** or **66a** for 48 h. Apoptosis was examined by flow cytometry (n = 3). Representative photographs from three independent experiments are displayed.

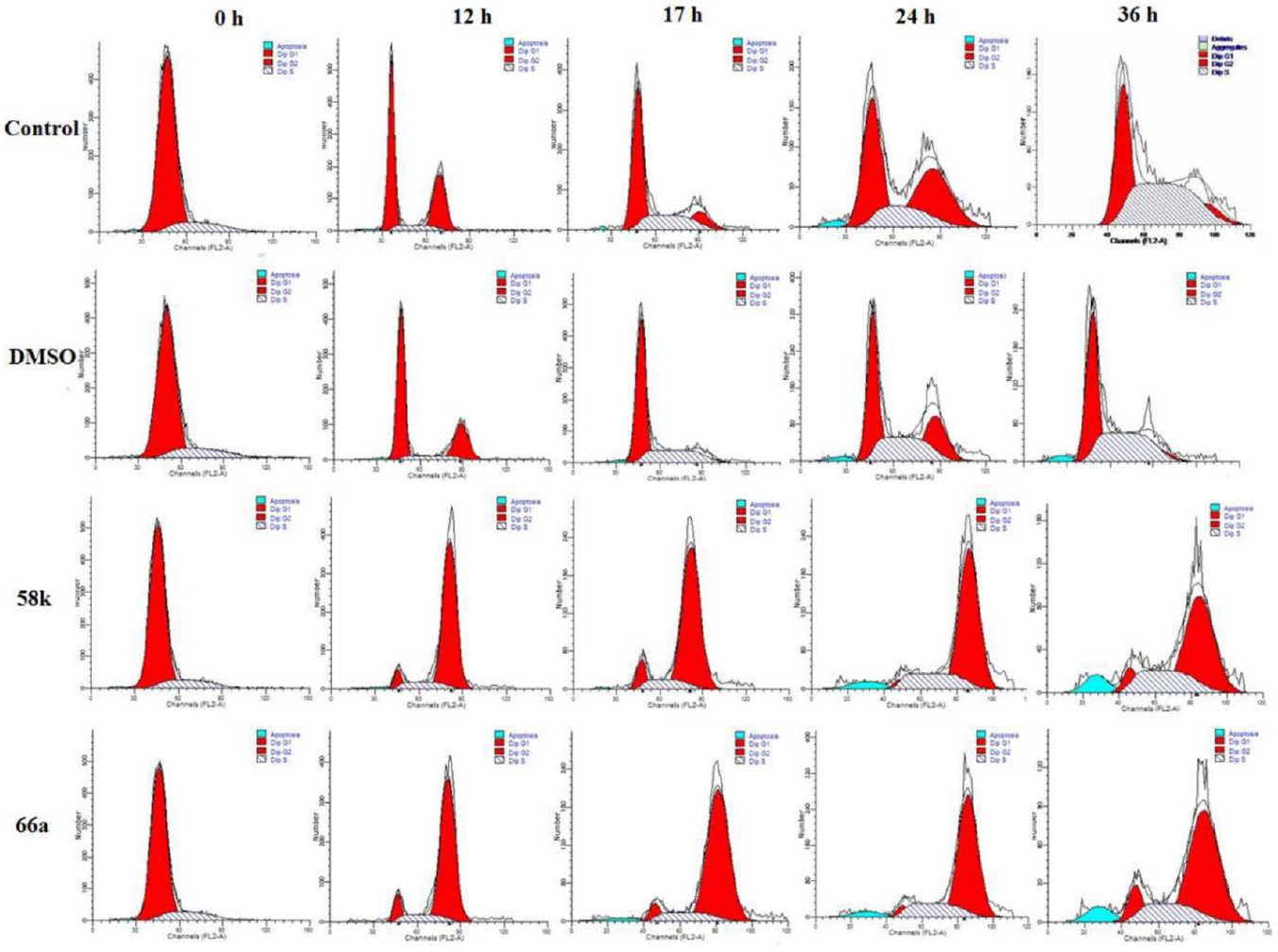

Figure 4. A549 cells treated with **58k** (5 μM) or **66a** (5 μM) for 0−36 h were assayed by flow cytometry after staining with PI. Cells untreated or treated with DMSO were used for comparison.

results indicated that thio-evodiamine derivatives showed higher inhibitory activity than the oxo-evodiamine derivatives against Top1-mediated DNA relaxation.

Next, the binding modes of compounds **58k** and **66c** were investigated by molecular docking and molecular dynamics (MD) simulations. Gold 5.0.1 and Desmond with the same

DOI: 10.1021/acs.jmedchem.5b00910
J. Med. Chem. 2015, 58, 6678−6696

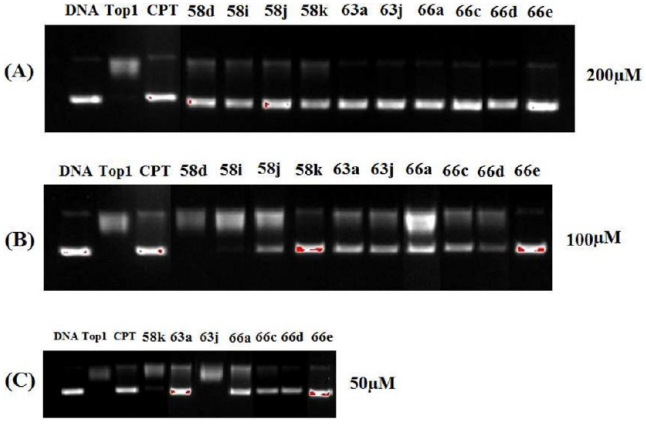

Figure 5. Top1 inhibitory activity of the evodiamine derivatives. (A) Inhibition of Top1 relaxation activity at 200 μM. Lane 1, supercoiled plasmid DNA; lane 2, DNA + Top1; lane 3, DNA + Top1 + CPT; and lanes 4−13, DNA + Top1 + evodiamine derivatives (**58d**, **58i**, **58j**, **58k**, **63a**, **63j**, **66a**, **66c**, **66d**, and **66e**, respectively). (B) Inhibition of Top1 relaxation activity at 100 μM. The lanes are the same as the assay at 200 μM. (C) Inhibition of Top1 relaxation activity at 50 μM. Lanes 4−10, DNA + Top1 + evodiamine derivatives (**58k**, **63a**, **63j**, **66a**, **66c**, **66d**, and **66e**, respectively).

parameters as those in our previous reports[34] were used for molecular modeling. As depicted in Figure 6, compounds **58k** and **66c** formed base-stacking interactions with the surrounding DNA base pairs. Their A-ring C10 hydroxyl groups formed a hydrogen bond with Glu356. Moreover, an additional hydrogen bond was observed between the E-ring C3 hydroxyl group of compound **58k** and Thr718. Evodiamine and its substituted analogues shared a unique "L type" conformation in the active site of Top1.[33] In contrast, oxo- and thio-evodiamine derivatives displayed "plannar" configuration in the binding site, which was beneficial to form stronger base-stacking interactions with surrounding DNA base pairs and thus enhance Top1 inhibitory activity.

Top2 Inhibitory Activity and the Binding Modes. Previously, Top2 was identified as another molecular target of evodiamine derivatives using the target prediction in combination with the enzymatic inhibitory assay.[34] To further evaluate the inhibitory effect of the oxo- and thio-evodiamine derivatives on Top2, representative compounds (i.e., **58d**, **58i**, **58j**, **58k**, **63a**, **63j**, **66a**, **66c**, **66d**, **66e**, and **66f**) were assayed. As shown in Figure 7, only compounds **58i**, **63j**, **66c**, and **66e** showed

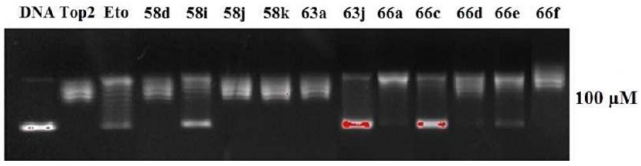

Figure 7. Top2 inhibitory activity of the evodiamine derivatives. (A) Inhibition of Top2 relaxation activity at 100 μM. Lane 1, supercoiled plasmid DNA; lane 2, DNA + Top2; lane 3, DNA + Top2 + etoposide; lanes 4−14, DNA + Top2 + evodiamine derivatives (**58d**, **58i**, **58j**, **58k**, **63a**, **63j**, **66a**, **66c**, **66d**, **66e**, and **66f**, respectively).

moderate to good Top2 inhibitory activity at a concentration of 100 μM. However, the other compounds were almost inactive at the same condition. In comparison with substituted evodiamine derivatives,[34] the new scaffolds showed decreased Top2 inhibitory activity, indicating that the new mechanism (targets) might be involved in their excellent antitumor activity.

To investigate the binding modes between evodiamine derivatives and Top2α, compounds **58i**, **66c**, and **66e** were subjected to molecular docking and molecular dynamic simulations. As depicted in Figure 8, all compounds were observed to be well-fitted into the ATP-binding domain of Top2α. The A-ring C10 hydroxyl group and D-ring C5 carbonyl group formed a hydrogen bond with Arg98 and Asn150, respectively. For compounds **58i** and **66e**, the E-ring C3 hydroxyl group formed coordination interaction with the Mg^{2+} ion and increased the binding energy with Top2α, which was consistent with the fact that the E-ring C3 hydroxyl was beneficial for increasing Top2α inhibitory activity.

Target Profiling Identified Compound 66c as the First Triple Top1/Top2/Tubulin Inhibitor. The oxo- and thio-evodiamine derivatives showed excellent *in vitro* antiproliferative activity, which was not consistent with their moderate Top1 and Top2α inhibitory activity. Thus, there might be additional targets for them. As a preliminary target profiling study, compounds **58k** and **66c** were screened against a panel of 31 antitumor targets at a concentration of 5 μM (Table S2). Interestingly, compounds **58k** and **66c** were found to be tubulin inhibitors with an inhibition rate of 48% and 63%, respectively. Furthermore, their IC_{50} values were determined using the concentration−activity assay with colchicine and vinorelbine as the positive controls (Figure S2). As shown in Figure 9, compounds **58k** and **66c** showed potent inhibitory activity on tubulin polymerization with IC_{50} values of 5.3 μM and 4.5 μM, respectively, which were more

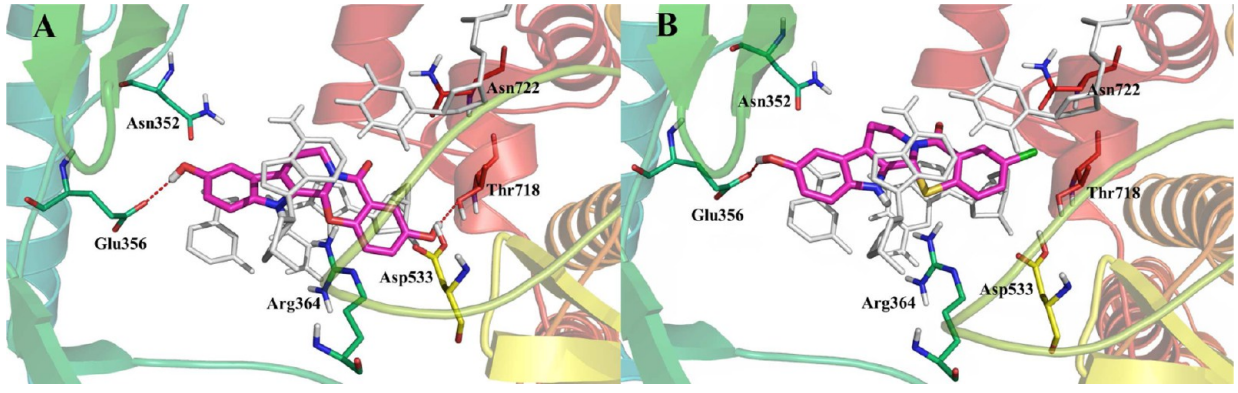

Figure 6. Schematic representation of the proposed binding mode for compounds **58k** (A) and **66c** (B) with Top1-DNA (PDB code: 1T8I). The figures were generated using Pymol (http://www.pymol.org/).

DOI: 10.1021/acs.jmedchem.5b00910
J. Med. Chem. 2015, 58, 6678−6696

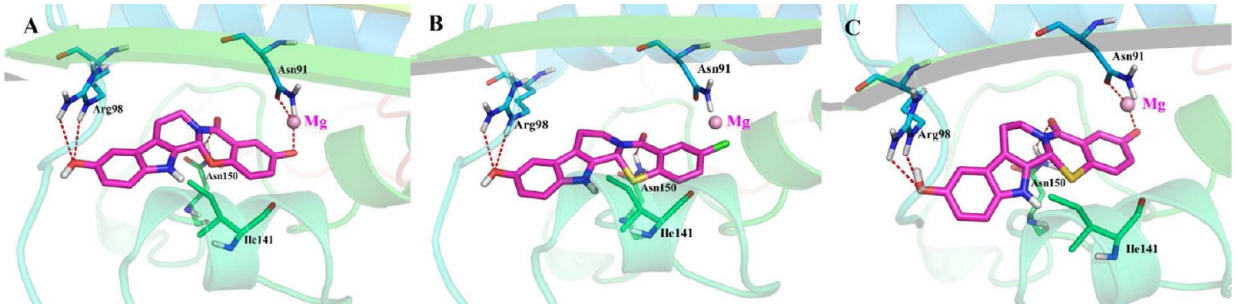

Figure 8. Schematic representation of the proposed binding mode for compounds **58i** (A), **66c** (B), and **66e** (C) in the ATP-binding domain of Top2α (PDB code: 1ZXM). The figures were generated using Pymol (http://www.pymol.org/).

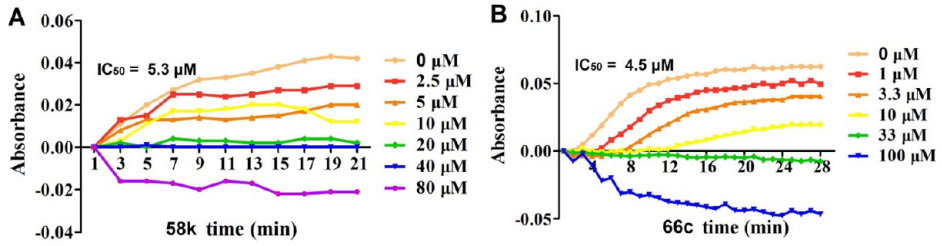

Figure 9. Tubulin inhibitory activity of compounds **58k** and **66c**. With treatment of different concentrations of **58k** (A) and **66c** (B), *in vitro* polymerization of tubulin at 37 °C was monitored continuously by recording the absorbance at 340 nm over 20 min. The data are the average of two independent experiments. Both compounds showed concentration-dependent inhibition of tubulin polymerization.

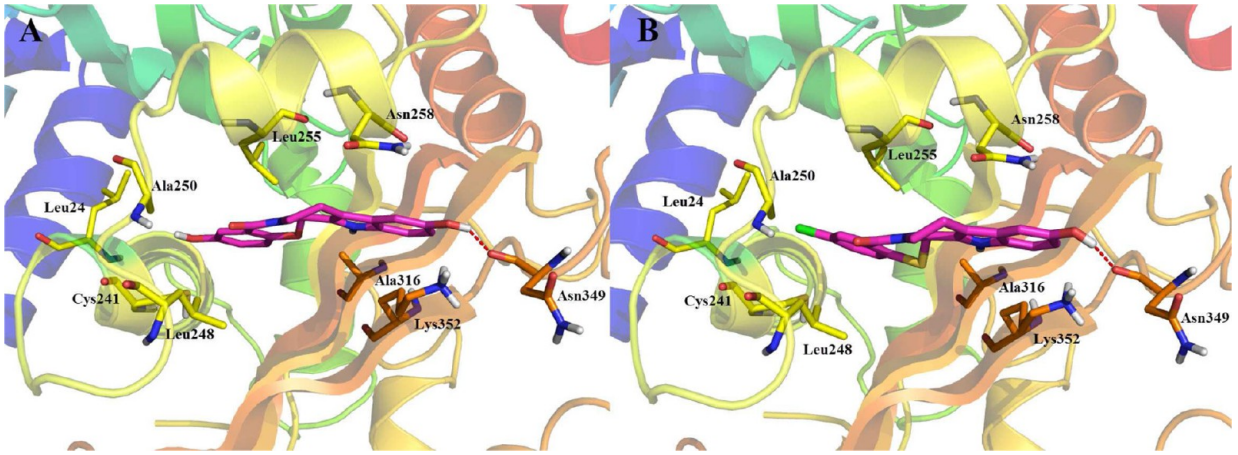

Figure 10. Schematic representation of the proposed binding mode for **58k** and **66c** in the colchicine binding domain of tubulin (PDB code: 1SA0). The figures were generated using Pymol (http://www.pymol.org/).

potent than colchicine (IC_{50} = 7.8 μM) and less potent than vinorelbine (IC_{50} = 2.0 μM). This assay confirmed that tubulin is another important antitumor target of oxo- and thio-evodiamine derivatives. Tubulin is an important target in antitumor drug discovery. Theoretically, combination therapy using topoisomerases and tubulin inhibitors is a promising strategy to enhance the final therapeutic outcome of cancer treatment.[46] Up to now, only dual Top1/tubulin inhibitors[47] and dual Top2/tubulin inhibitors[48] were reported. On the basis of the above assays, compound **58k** is a dual Top1/tubulin inhibitor. Interestingly, to the best of our knowledge, compound **66c** is the first-in-class triple Top1/Top2/tubulin inhibitor.

To clarify the interactions between compounds **58k** and **66c** with tubulin, molecular docking was performed. Similar to our previous report,[49] the X-ray crystal structure of the DAMA–colchicine–tubulin complex (PDB code: 1SA0) was used as the tubulin protein template. As depicted in Figure 10, both compounds were observed to be well-fitted into the colchicine-binding domain of tubulin. The C, D, and E rings inserted deeply into the hydrophobic pocket and formed hydrophobic interactions with surrounding residues such as Leu248, Val238, Lys254, and Ala250. Moreover, the A-ring C10 hydroxyl group of **58k** and **66c** formed a hydrogen bond with the carbonyl group of Asn349.

Inhibition of Tumor Growth of A549 and HCT116 Tumor Xenografts in Nude Mice. To further investigate the *in vivo* antitumor potency of the oxo- and thio-evodiamine derivatives, two xenograft nude mice models (A549 and HCT116 xenograft models) were prepared according to our previous report.[34] Representative compounds were chosen according to their chemical structures and *in vitro* antiproliferative activity. First, compounds **58g**, **58k**, and **66a** were tested in the A549 xenograft model at a dose of 2 mg/kg. After administering intraperitoneally (ip) for five consecutive days,

DOI: 10.1021/acs.jmedchem.5b00910
J. Med. Chem. 2015, 58, 6678–6696

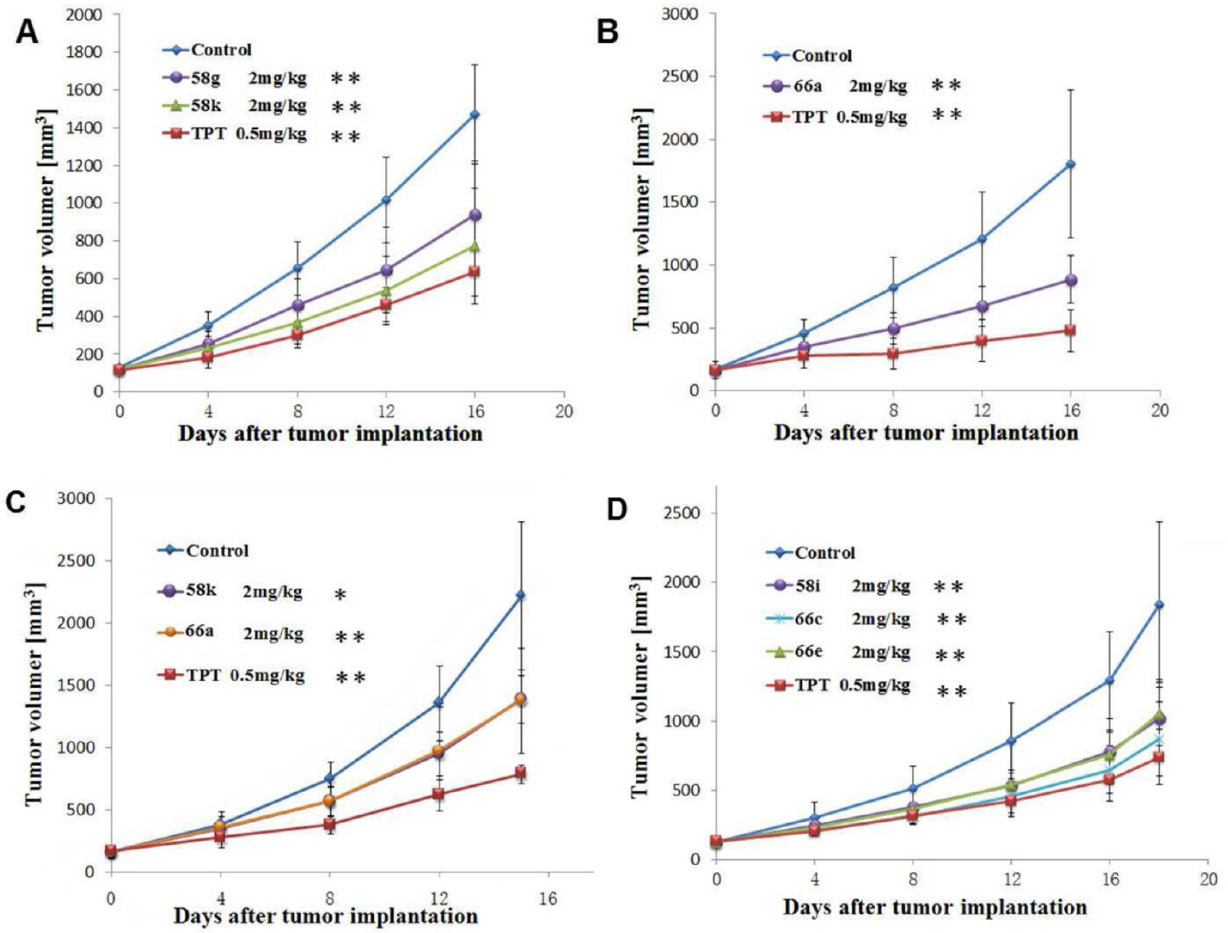

Figure 11. Antitumor efficacy of oxo- and thio-evodiamine derivatives in the xenograft models. **TPT** at the dose of 0.5 mg/kg was used for the positive control. (A) The efficacy of compounds **58g** and **58k** in the A549 xenograft model at a dose of 2 mg/kg; (B) the efficacy of compound **66a** in the A549 xenograft model at a dose of 2 mg/kg; (C) the efficacy of compounds **58k** and **66a** in the HCT116 xenograft model at a dose of 2 mg/kg; and (D) the efficacy of compounds **58i**, **66c**, and **66e** in the HCT116 xenograft model at a dose of 2 mg/kg. Data are presented as the mean ± SEM; $n = 6$ nude mice per group: (*) $P < 0.05$, (**) $P < 0.01$, versus the control group, determined with Student's t test.

significant tumor growth inhibition was observed (Figure 11A and B, $p < 0.01$). Among them, 10-hydroxyl thio-evodiamine (**66a**) showed the most potent *in vivo* antitumor potency with the tumor growth inhibition rate of 48%. Moreover, all of the compounds were observed to be well tolerated during the test, and no significant loss of body weight was observed, indicating that their toxicity is low (Figure S3). In contrast, TPT at a dose of 0.5 mg/kg caused significant decrease of body weight (Figure S3). In the HCT116 xenograft model, all of the tested compounds (i.e., **58k**, **66a**, **58i**, **66c**, and **66e**) showed remarkable tumor growth inhibition at a dose of 2 mg/kg. In particular, 3-chloro-10-hydroxyl thio-evodiamine (**66c**) showed the best *in vivo* potency with low toxicity. Generally, the thio-evodiamine derivatives showed better *in vivo* antitumor potency compared with that of the corresponding oxo-evodiamine derivatives.

CONCLUSIONS

In summary, evodiamine-inspired scaffold diversity was investigated by the generation of 11 novel scaffolds. The significance of this work includes (1) providing an in-depth understanding of the scaffold SAR of evodiamine; (2) identifying a series of highly potent antitumor molecules with promising features as antitumor candidates; and (3) discovering the first-in-class Top1/Top2/tubulin inhibitor and preliminarily highlighting the advantage of this kind of triple inhibition. Notably, compound **66c** is a multitargeting antitumor candidate with excellent *in vitro* and *in vivo* antitumor potency. Further antitumor mechanism and structural optimization are in progress.

EXPERIMENTAL SECTION

Chemistry. *General Methods.* ^{1}H NMR and ^{13}C NMR spectra were recorded on Bruker AVANCE300, AVANCE500, or AVANCE600 spectrometers (Bruker Company, Germany), using TMS as an internal standard and $CDCl_3$ or DMSO-d_6 as solvents. Chemical shifts are given in ppm (δ). Elemental analyses were performed with a MOD-1106 instrument and were consistent with theoretical values within 0.4%. The mass spectra were recorded on an Esquire 3000 LC-MS mass spectrometer. Silica gel thin-layer chromatography was performed on precoated plates GF-254 (Qingdao Haiyang Chemical, China). Purity of the compounds was analyzed by HPLC (Agilent Technologies 1260 Infinity) using 40:60 MeOH/H_2O as the mobile phase with a flow rate of 0.8 mL/min on a C18 column (Aglilent 20RBA × SB-C18, 5 μm, 4.6 mm × 150 mm). All compounds exhibited greater than 95% purity. All solvents and reagents were analytically pure, and no further purification was needed. All starting materials were commercially available.

*9-Methoxy-13-methyl-7,12,12b,13-tetrahydrothieno[3″,2″:4′,5′]-pyrimido[1′,2′:1,2]pyrido[3, 4-b]indol-4(6H)-one (**12a**).* A solution of intermediates **8a** (0.15 g, 0.81 mmol) and **11** (0.15 g, 0.81 mmol) in DCM (10 mL) was stirred overnight at room temperature. Then, target

DOI: 10.1021/acs.jmedchem.5b00910
J. Med. Chem. 2015, 58, 6678−6696

compound **12a** was precipitated from the solution and washed by DCM to give a yellow solid (0.2 g, 72.9%). ^{1}H NMR (DMSO-d_6, 600 MHz) δ: 2.62 (s, 3H), 2.74−2.85 (m, 1H), 3.12−3.17 (m, 1H), 3.77 (s, 3H), 4.48−4.51 (m, 1H), 6.05 (s, 1H), 6.78 (dd, J = 2.5 Hz, 8.8 Hz, 1H), 7.01 (d, J = 2.3 Hz, 1H), 7.03 (d, J = 5.2 Hz, 1H), 7.26 (d, J = 8.8 Hz, 1H), 7.84 (d, J = 5.2 Hz, 1H), 11.11 (s, 1H); ^{13}C NMR (DMSO-d_6, 150 MHz,) δ: 162.12, 155.73, 154.16, 133.83, 132.50, 130.13, 126.86, 121.12, 116.77, 113.07, 113.07, 112.89, 112.44, 101.01, 70.89, 56.16, 36.43, 20.67. MS (ESI, positive) m/z calcd for $C_{18}H_{18}N_3O_2S$ (M + H): 340.11; found 340.45. Anal. ($C_{18}H_{17}N_3O_2S$) C, H, N. HPLC purity: 97.7%. The synthetic method for compounds **12b** and **15** was similar to the synthesis of compound **12a**.

*9-Hydroxy-13-methyl-7,12,12b,13-tetrahydrothieno[3″,2″:4′,5′]-pyrimido[1′,2′:1,2]pyrido[3,4-b]indol-4(6H)-one (**12c**).* To a stirred solution of compound **12a** (0.2 g, 0.59 mmol) in DCM (20 mL), BBr_3 (0.2 mL) was added in one portion and stirred for 6 h at −78 °C. After the addition of methanol (0.2 mL) and DCM (30 mL), the solution was washed with saturated $NaHCO_3$ aqueous solution (60 mL) and brine (40 mL) and dried over Na_2SO_4, and the solvent was removed under reduced pressure. The residue was purified by silica gel column chromatography (Hexane: EtOAc = 2:1) to give compound **12c** (0.09 g, yield 47.4%) as a yellow solid. ^{1}H NMR (DMSO-d_6, 600 MHz) δ: 2.62 (s, 3H), 2.73−2.74 (m, 1H), 3.11−3.15 (m, 1H), 4.45−4.49 (m, 1H), 6.02 (s, 1H), 6.65 (dd, J = 8.5 Hz, 2.3 Hz, 1H), 6.79 (d, J = 2.3 Hz, 1H), 7.02 (d, J = 5.3 Hz, 1H), 7.16 (d, J = 8.3 Hz, 1H), 7.82 (d, J = 5.2 Hz, 1H), 8.70 (s, 1H), 10.93 (s, 1H). MS (ESI, positive) m/z calcd for $C_{17}H_{16}N_3OS$ (M + H): 326.09; found 326.09. Anal. ($C_{17}H_{15}N_3OS$) C, H, N. HPLC purity: 97.9%. The synthetic method for compounds **26b**, **29c**, **47**, and **54b** was similar to the synthesis of compound **12c**.

*9-Methoxy-13-methyl-7,12,12b,13-tetrahydrothieno[2″,3″:4′,5′]-pyrimido[1′,2′:1,2]pyrido[3,4-b]indol-4(6H)-one (**15**).* Yellow solid: 0.06 g (yield 65.7%). ^{1}H NMR (DMSO-d_6, 600 MHz) δ: 2.72 (s, 3H), 2.77−2.79 (m, 2H), 3.04−3.11 (m, 1H), 3.75 (s, 3H), 4.52 (d, J = 12.2 Hz, 1H), 6.11 (s, 1H), 6.76 (dd, J = 2.4 Hz, 8.8 Hz, 1H), 6.93 (d, J = 5.6 Hz, 1H), 6.99 (d, J = 2.2 Hz, 1H), 7.06 (d, J = 5.6 Hz, 1H), 7.26 (d, J = 8.7 Hz, 1H), 11.10 (s, 1H). ^{13}C NMR (DMSO-d_6, 150 MHz) δ: 36.89, 40.03, 55.31, 71.68, 98.71, 102.19, 108.97, 110.25, 111.58, 118.24, 127.42, 131.69, 133.42, 134.05, 154.04, 154.12, 161.23. MS (ESI, negative) m/z calcd for $C_{18}H_{18}N_3O_2S$ (M + H): 338.11; found 338.00. Anal. ($C_{18}H_{17}N_3O_2S$) C, H, N. HPLC purity: 98.1%.

*9-Methoxy-13-methyl-7,12,12b,13-tetrahydro-4H,6H-thieno-[3″,4″:4′,5′]pyrimido[1′,2′:1,2]pyrido[3,4-b]indol-4-one (**26a**).* Methyl acrylate (99.16 mL, 1.1 mol) was added slowly to a solution of methyl 2-mercaptoacetate (91 mL, 1 mol) and piperidine (2 mL) maintaining the temperature at 50 °C for 2 h. Then, excess methyl acrylate and piperidine were distilled off under high vacuum to yield intermediate **18** (192 g, 99%) as a colorless viscous oil, which was used directly for the next step without further purification. ^{1}H NMR ($CDCl_3$, 600 MHz) δ: 2.63 (d, J = 7.2 Hz, 2H), 2.89 (d, J = 7.2 Hz, 2H), 3.24 (s, 2H), 3.68 (s, 3H), 3.72 (s, 3H).

To a solution of NaH (60% in mineral oil, 13.24 g, 331 mmol) in THF, intermediate **18** (58 g, 300 mmol) in dry THF (800 mL) was added slowly within 4 h, and the reaction mixture was refluxed for 5 h. Then, the solvent was concentrated under reduced pressure, and H_2O (300 mL) was added to the residue. The pH value of the solution was adjusted to 1 by cold HCl solution and extracted with DCM (100 mL × 3). The combined organic layers were dried over $MgSO_4$ and concentrated under vacuum. The residue was purified by flash chromatography eluting with hexane to yield intermediate **19** (17 g, 35%) as colorless viscous oil. ^{1}H NMR ($CDCl_3$, 600 MHz) δ: 3.17−3.82 (m, 6 H), 10.94 (s, 1H).

A mixture of intermediate **19** (17 g, 106 mmol), hydroxylamine hydrochloride (17 g, 244 mmol), and barium carbonate (48.16 g, 244 mmol) was refluxed for 12 h in MeOH (800 mL). Then, the mixture was cooled and filtered. The solvent was concentrated under reduced pressure. The residue was suspended in water (300 mL) and extracted by EtOAc (100 mL × 3). The combined organic layers were dried over $MgSO_4$ and concentrated to yield intermediate **20** (18.3 g, 98%) as a viscous oil, which was used directly for the next step without further purification. ^{1}H NMR ($CDCl_3$, 600 MHz) δ: 3.14−4.11 (m, 7H), 8.17 (m, 1H).

To a solution of intermediate **20** (18.3 g, 104 mmol) in dry ether (200 mL) and MeOH (50 mL), HCl (1 M solution in ether, 125 mL) was added slowly, and the mixture was stirred at room temperature for 24 h under argon protection. After reaction, the solid was filtered from the solution and washed with cold ether to afford intermediate **21** in hydrochloride form (18.2 g, 91%). ^{1}H NMR (DMSO-d_6, 600 MHz) δ: 3.86 (s, 3H), 7.22 (d, J = 2.4 Hz, 1H), 8.37 (d, J = 3.2 Hz, 1H). MS (ESI, positive) m/z calcd for $C_6H_8NO_2S$ (M + H): 158.02; found 158.34.

Starting from intermediate **21**, intermediate **24** was obtained according to the method reported by the literature.[50] ^{1}H NMR (DMSO-d_6, 600 MHz) δ: 2.73 (s, 3H), 3.76 (s, 3H), 5.85 (s, 1H), 5.98 (d, J = 3.3 Hz, 1H), 8.16 (d, J = 3.5 Hz, 1H).

To a small microwave tube was added intermediate **8c** (0.25 g, 1.16 mmol), **24** (0.2 g, 1.16 mmol), $POCl_3$ (0.14 mL, 1.5 mmol), and dry toluene (20 mL). The mixture was irradiated at 130 °C for 45 min in a Biotage microwave cavity. After the reaction, the solvent was evaporated, and the residue was dissolved in EtOH (15 mL). Then, $NaBH_4$ (0.13 g, 3.51 mmol) was added, and the mixture was stirred for 2 h at 0 °C. After the reaction, the solvent was evaporated, and the residue was purified using flash column chromatography (silica gel, hexane/EtOAc = 3:1) to afford **26a** as a brown solid (0.17 g, yield: 43.1%). ^{1}H NMR (DMSO-d_6, 600 MHz) δ: 2.75 (s, 3H), 2.79−2.83 (m, 2H), 3.09−3.16 (m, 1H), 3.74 (s, 3H), 4.61−4.64 (m, 1H), 5.98 (s, 1H), 6.72 (d, J = 3.1 Hz, 1H), 6.74 (dd, J = 2.4 Hz, 8.8 Hz, 1H), 6.96 (d, J = 2.5 Hz, 1H), 7.24 (d, J = 8.6 Hz, 1H), 8.06 (d, J = 3.1 Hz, 1H), 10.88 (s, 1H). MS (ESI, positive) m/z calcd for $C_{18}H_{18}N_3O_2S$ (M + H): 340.11; found 340.24. Anal. ($C_{18}H_{17}N_3O_2S$) C, H, N. HPLC purity: 98.6%. The synthetic method for compounds **26b**, **29a**, **29b**, **32**, **46**, and **54a** was similar to that of compound **26a**.

*9-Hydroxy-13-methyl-7,12,12b,13-tetrahydro-4H,6H-thieno-[3″,4″:4′,5′]pyrimido[1′,2′:1,2]pyrido[3,4-b]indol-4-one (**26b**).* Yellow solid: 0.25 g (yield 49.5%). ^{1}H NMR (DMSO-d_6, 600 MHz) δ: 2.64−2.68 (m, 1H), 2.76 (s, 3H), 2.77−2.80 (m, 1H), 3.08−3.13 (m, 1H), 4.61 (dd, J = 4.7 Hz, 12.8 Hz, 1H), 5.96 (s, 1H), 6.62 (dd, J = 2.1 Hz, 8.7 Hz, 1H), 6.70 (d, J = 3.1 Hz, 1H), 6.74 (s, 1H), 7.14 (d, J = 8.8 Hz, 1H), 8.05 (d, J = 3.0 Hz, 1H), 8.66 (s, 1H), 10.70 (s, 1H). ^{13}C NMR (DMSO-d_6, 150 MHz) δ: 20.61, 38.03, 41.34, 72.24, 102.91, 104.88, 111.33, 112.81, 112.91, 126.86, 127.30, 130.44, 131.70, 131.76, 148.51, 151.44, 162.11. MS (ESI, positive) m/z calcd for $C_{17}H_{16}N_3O_2S$ (M + H): 326.09; found 326.33. Anal. ($C_{17}H_{15}N_3O_2S$) C, H, N. HPLC purity: 97.8%.

*9-Methoxy-3,13-dimethyl-3,6,7,12,12b,13-hexahydro-4H-pyrrolo[3″,2″:4′,5′]pyrimido[1′,2′:1,2]pyrido[3,4-b]indol-4-one (**29b**).* Yellow solid: 0.24 g (yield 43.5%). ^{1}H NMR (DMSO-d_6, 600 MHz) δ: 2.27 (s, 3H), 2.67−2.72 (m, 1H), 2.82−2.85 (m, 1H), 3.07−3.18 (m, 1H), 3.76 (s, 3H), 3.84 (s, 3H), 4.44−4.48 (m, 1H), 5.84 (s, 1H), 5.86 (d, J = 2.7 Hz, 1H), 6.76 (dd, J = 8.8 Hz, 2.5 Hz, 1H), 6.93 (d, J = 2.7 Hz, 1H), 7.01 (d, J = 2.4 Hz, 1H), 7.24 (dd, J = 8.8 Hz, 0.4 Hz, 1H), 11.14 (s, 1H). ^{13}C NMR (DMSO-d_6, 150 MHz) δ: 20.98, 36.23, 36.95, 39.16, 56.15, 71.19, 99.21, 101.02, 112.14, 112.62, 112.96, 115.92, 126.73, 129.34, 130.69, 132.58, 144.38, 154.06, 160.60. MS (ESI, positive) m/z calcd for $C_{19}H_{21}N_4O_2$ (M + H): 337.16; found 337.10. Anal. ($C_{19}H_{20}N_4O_2$) C, H, N. HPLC purity: 97.8%.

*13-Methyl-7,12,12b,13-tetrahydrofuro[3″,2″:4′,5′]pyrimido-[1′,2′:1,2]pyrido[3,4-b]indol-4(6H)-one (**32**).* The synthetic method for intermediate **31** was similar to that of intermediate **24**. ^{1}H NMR (DMSO-d_6, 600 MHz) δ: 2.79 (d, J = 5.2 Hz, 3H), 3.69 (s, 3H), 5.70 (s, 1H), 6.42 (d, J = 1.9 Hz, 1H), 7.62 (d, J = 1.9 Hz, 1H).

According to the synthetic method of compound **26a**, compound **32** was obtained as a yellow solid: 0.11 g (yield 36.3%). ^{1}H NMR (DMSO-d_6, 600 MHz) δ: 2.46 (s, 3H), 2.73−2.77 (m, 1H), 2.87 (d, J = 15.0 Hz, 1H), 3.12−3.17 (m, 1H), 4.39−4.43 (m, 1H), 6.0 (s, 1H), 6.67 (d, J = 2.0 Hz, 1H), 7.03 (dt, J = 7.11 Hz, 0.9 Hz, 1H), 7.14 (dt, J = 7.1 Hz, 1.1 Hz, 1H), 7.38 (d, J = 8.2 Hz, 1H), 7.52 (d, J = 7.8 Hz, 1H), 7.85 (d, J = 2.0 Hz, 1H), 11.34 (s, 1H). ^{13}C NMR (DMSO-d_6, 150 MHz) δ: 19.86, 34.82, 38.95, 69.92, 105.02, 111.56, 111.88, 118.40, 118.83, 121.93, 125.64, 128.21, 134.42, 136.68, 145.55, 148.14, 157.43. MS (ESI,

DOI: 10.1021/acs.jmedchem.5b00910
J. Med. Chem. 2015, 58, 6678−6696

positive) m/z calcd for $C_{17}H_{16}N_3O_2$ (M + H): 294.12; found 294.12. Anal. ($C_{17}H_{15}N_3O_2$) C, H, N. HPLC purity: 98.8%.

*13b-Hydroxy-10-methoxy-7,8,13,13b-tetrahydro-5H-benzo[1,2]-indolizino[8,7-b]indol-5-one (**36a**).* The synthetic method for compounds **36a** and **36b** was according to the procedure reported by You's group.[42] To a solution of 5-methoxytryptamine (1.9 g, 10 mmol) in toluene (50 mL), phthalic anhydride (1.63 g, 11 mmol) was added. Then, the solution was heated to reflux. After the reaction was completed (monitored by TLC), the solvent was evaporated under reduced pressure. The residue was purified by recrystallization in EtOAc. The resulting solid (2.03 g, 7 mmol) was dissolved in DCM (50 mL), and then TfOH (5.25 g, 35 mmol) was added slowly at 0 °C. After 30 min, the reaction mixture was quenched with water (50 mL) followed by the addition of $NaHCO_3$ (10 g). The resulting suspension was filtered through a pad of Celite, and the collected solid was washed with ether and dried to yield compound **36a** (1.56 g, yield 48.8%) as a yellow solid. ^{1}H NMR (DMSO-d_6, 600 MHz) δ: 2.65−2.81 (m, 2H), 3.42−3.52 (m, 1H), 3.73 (s, 3H), 4.41 (dd, J = 13.1 Hz, 5.0 Hz, 1H), 6.76 (dd, J = 8.8 Hz, 2.5 Hz, 1H), 6.93 (d, J = 2.4 Hz, 1H), 7.25 (s, 1H), 7.28 (s, 1H), 7.52−7.58 (m, 1H), 7.67−7.75 (m, 2H), 8.31 (d, J = 7.6 Hz, 1H), 11.36 (s, 1H). ^{13}C NMR (DMSO-d_6, 150 MHz) δ: 21.7, 35.1, 55.4, 84.2, 100.6, 108.8, 112.4, 112.5, 122.8, 123.7, 125.9, 129.6, 130.4, 131.6, 132.5, 133.7, 147.1, 153.4, 166.5. MS (ESI, positive) m/z calcd for $C_{19}H_{17}N_2O_3$ (M + H): 321.12; found 321.12. Anal. ($C_{19}H_{16}N_2O_3$) C, H, N. HPLC purity: 97.5%.

*10-Methoxy-7,8,13,13b-tetrahydro-5H-benzo[1,2]indolizino[8,7-b]indol-5-one (**36b**).* To a solution of compound **36a** (64 mg, 0.2 mmol) in dioxane (4 mL) was successively added catalyst **38** (8.8 mg, 5 mol %) and intermediate **37** (123.6 mg, 0.2 mmol), then the reaction mixture was stirred at room temperature. After the reaction was completed (monitored by TLC), saturated $NaHCO_3$ solution was added. The organic layer was separated, and the aqueous layer was extracted with EtOAc. The combined organic extract was washed with brine solution, dried over anhydrous Na_2SO_4, filtrated, and then concentrated. The residue was purified by silica gel column chromatography (EtOAc/hexane = 1:4) to afford **36b** as a white solid: 0.53 g (yield 86.9%). ^{1}H NMR (DMSO-d_6, 600 MHz) δ: 2.64−2.69 (m, 1H), 2.80 (dd, J = 15.2 Hz, 4.3 Hz, 1H), 3.33−3.38 (m, 1H), 3.73 (s, 3H), 4.60 (dd, J = 13.0 Hz, 6.1 Hz, 1H), 6.03 (s, 1H), 6.73 (dd, J = 8.8 Hz, 2.5 Hz, 1H), 6.91 (d, J = 2.3 Hz, 1H), 7.27 (d, J = 8.8 Hz, 1H), 7.54 (t, J = 7.4 Hz, 1H), 7.71 (t, J = 7.4 Hz, 1H), 7.74 (d, J = 7.6 Hz, 1H), 8.27 (d, J = 7.7 Hz, 1H), 11.17 (s, 1H). ^{13}C NMR (DMSO-d_6, 150 MHz) δ: 21.52, 36.78, 55.29, 56.73, 100.15, 107.00, 111.53, 112.00, 123.22, 123.86, 131.49, 131.73, 143.70, 153.41, 167.22. MS (ESI, positive) m/z calcd for $C_{19}H_{17}N_2O_2$ (M + H): 305.12; found 305.37. Anal. ($C_{19}H_{16}N_2O_2$) C, H, N. HPLC purity: 96.3%.

*11-Methoxy-15-methyl-7,8,9,14,14b,15-hexahydro-5H-indolo-[2′,3′:3,4]azepino[2,1-b]quinazolin-5-one (**46**).* To a solution of ε-caprolactam (15.2 g, 133 mmol) in DCM (400 mL), PCl_5 (55.2 g, 265 mmol) was added, and the mixture was stirred at 0 °C for 30 min. Then, anhydrous ZnI_2 (1.53 g, 4.79 mmol) was added, and the reaction was protected under N_2. The reaction mixture was slowly cooled to room temperature, while Br_2 (42.4 g, 265 mmol) was added dropwise over the course of 30 min. The mixture was stirred at room temperature for 6 h and then poured into ice−water (300 mL). The aqueous layer was extracted with DCM (3 × 100 mL), and the combined organic layers were washed with 0.50 M aq $NaHSO_3$ (3 × 200 mL) and brine (400 mL), dried over $MgSO_4$, and concentrated to yield a crude solid. The solid was suspended in water, filtered, and washed with water and Et_2O to give 3,3-dibromoazepan-2-one (intermediate **40**, 25.3 g, yield 70.2%) as a white solid. ^{1}H NMR ($CDCl_3$, 600 MHz) δ: 1.67−1.73 (m, 2H), 1.94−2.02 (m, 2H), 2.72−2.77 (m, 2H), 3.39 (dd, J = 10.3 Hz, 5.8 Hz, 2H), 6.91 (bs, 1 H).

A solution of 3,3-dibromoazepan-2-one (15.7 g, 57.9 mmol) in piperidine (140 mL) was refluxed for 4.5 h under N_2. Then, the solution was cooled to room temperature and washed with aq $NaHSO_3$ (0.50 M, 200 mL). The aqueous phase was extracted with $CHCl_3$ (3 × 100 mL), and the combined organic layers were washed with brine (300 mL), dried over $MgSO_4$, and concentrated to afford a brown, oily solid that crystallized upon standing. The resulting solid was suspended in water, filtered, and washed with water and Et_2O to give 3-(piperidin-1-yl)-1,5,6,7-tetrahydro-2*H*-azepin-2-one (intermediate **41**, 10.3 g, yield 91.4%) as a white solid. ^{1}H NMR ($CDCl_3$, 600 MHz) δ: 1.48−1.54 (m, 2 H), 1.62−1.69 (m, 4 H), 1.76 (q, J = 6.8 Hz, 2 H), 2.15 (q, 2 H, J = 7.2 Hz), 2.78 (t, J = 5.3 Hz, 4 H), 3.22 (q, J = 6.5 Hz, 2 H), 5.06 (t, J = 7.6 Hz, 1 H), 6.51 (bs, 1 H).

Intermediates **41** (390 mg, 20.1 mmol) and **42** (440 mg, 25.2 mmol) were added in anhydrous EtOH (50 mL) and H_2SO_4 (1 mL), and the mixture was refluxed for 5 h. Then, the solution was cooled to room temperature, and the resulting black solid was filtered, washed with water and Et_2O, preadsorbed on SiO_2, and purified by chromatography on SiO_2 (DCM/MeOH = 100:2) to yield 7-methoxy-3,4,5,10-tetrahydroazepino[3,4-*b*]indol-1(2*H*)-one (intermediate **43**, 246 mg, yield 53.3%) as a light orange solid. ^{1}H NMR (DMSO-d_6, 600 MHz) δ: 2.01 (d, J = 5.1 Hz, 1H), 2.97 (t, J = 6.1 Hz, 2H), 3.27−3.30 (m, 2H), 3.75 (s, 3H), 6.84 (dd, J = 8.8 Hz, 2.3 Hz, 1H), 6.97 (s, 1H), 7.27 (d, J = 8.8 Hz, 1H), 7.91 (s, 1H), 10.98 (s, 1H). MS (ESI, positive) m/z calcd for $C_{13}H_{15}N_2O_2$ (M + H): 231.11; found 231.15.

According to the synthetic method of compound **26a**, compound **46** was obtained as a yellow solid: 0.25 g (yield 37.5%). ^{1}H NMR (DMSO-d_6, 600 MHz) δ: 1.91−1.94 (m, 2H), 2.74−2.84 (m, 2H), 3.14−3.19 (m, 1H), 3.35 (s, 3H), 3.71 (s, 3H), 4.61−4.65 (m, 1H), 6.28 (s, 1H), 6.62 (dd, J = 8.6 Hz, 1.5 Hz, 1H), 6.72−6.76 (m, 1H), 6.88 (s, 1H), 6.97 (d, J = 8.3 Hz, 1H), 7.14 (d, J = 8.4 Hz, 1H), 7.42−7.45 (m, 1H), 7.60 (d, J = 7.6 Hz, 1H), 10.10 (s, 1H). ^{13}C NMR (DMSO-d_6, 150 MHz) δ: 21.96, 26.61, 37.64, 45.86, 55.26, 72.03, 99.42, 111.07, 112.22, 112.27, 113.94, 116.27, 117.49, 127.62, 128.10, 129.34, 133.22, 136.82, 146.33, 153.20, 162.10. MS (ESI, positive) m/z calcd for $C_{21}H_{22}N_3O_2$ (M + H): 348.17; found 348.50. Anal. ($C_{21}H_{21}N_3O_2$) C, H, N. HPLC purity: 96.9%.

*11-Methoxy-15-methyl-8,9,14b,15-tetrahydrobenzofuro-[2′,3′:3,4]azepino[2,1-b]quinazolin-5(7H)-one (**54a**).* The synthesis of intermediate **49** was according to the procedure described by the literature.[51] A mixture of enamine **41** (1.12 g, 6.2 mmol) and quinone (0.67 g, 6.2 mmol) in acetone (10 mL) was stirred for 6 h at 20 °C. After the reaction, the precipitate was filtered out and washed with acetone to give intermediate **49** as a brown solid (0.87 g, yield 47.3%). ^{1}H NMR (DMSO-d_6, 600 MHz) δ: 1.43 (m, 7H), 2.20 (m, 1H), 2.64 (m, 4H), 3.02 (m,1H), 3.17 (m, 1H), 3.64 (dd, J = 9.2 Hz, 7.2 Hz, 1H), 6.49−6.59 (m, 3H), 7.96 (s, 1H), 8.79 (s, 1H).

Intermediate **49** (0.8 g, 2.6 mmol) was added to AcOH (30 mL), and the solution was refluxed for 4 h. After reaction, the solvent was evaporated under reduced pressure. Then, 20 mL of water was added to the residue, and the pH value was adjusted to 7 by saturated $NaHCO_3$ solution. DCM (30 mL × 3) was added, and the aqueous layer was extracted three times. The combined organic phase was washed with water, dried over $MgSO_4$, and concentrated under vacuum to get a viscous residue. The residue was purified by chromatography on SiO_2 (DCM/MeOH = 100:2) to yield intermediate **50** (0.27 g, yield 46.6%) as a pale solid. ^{1}H NMR (DMSO-d_6, 600 MHz) δ: 1.87 (q, J = 5.5 Hz, 2H), 2.58 (t, J = 6.4 Hz, 2H), 3.20−3.23 (m, 2H), 5.89 (s, 1H), 6.66 (dd, J = 8.7, 2.7 Hz, 1H), 6.73 (d, J = 2.7 Hz, 1H), 7.09 (d, J = 8.7 Hz, 1H), 9.42 (s, 1H).

To a stirring solution of compound **50** (0.25 g, 1.08 mmol) and K_2CO_3 (0.2 g, 1.08 mmol) in EtOH (20 mL), CH_3I (0.14 mL, 2.16 mmol) was added, and the mixture was heated at 60 °C for 5 h. Then, the solvent was removed under reduced pressure. The residue was purified by silica gel column chromatography (DCM/MeOH = 100:3) to afford compound **51** as a white solid (0.22 g, yield 88.1%). ^{1}H NMR (DMSO-d_6, 600 MHz) δ: 2.01 (d, J = 5.1 Hz, 1H), 2.97 (t, J = 6.1 Hz, 2H), 3.27−3.30 (m, 2H), 3.75 (s, 3H), 6.84 (dd, J = 8.8, 2.3 Hz, 1H), 6.97 (s, 1H), 7.27 (d, J = 8.8 Hz, 1H), 7.91 (s, 1H), 10.98 (s, 1H).

According to the synthetic method of compound **26a**, compound **54a** was obtained as a white solid: 0.33 g (yield 64.8%). ^{1}H NMR ($CDCl_3$, 600 MHz) δ: 1.92−2.06 (m, 1H), 2.25−2.37 (m, 1H), 2.71−2.75 (m, 2H), 3.06−3.14 (m, 1H), 3.36 (s, 3H), 3.81 (s, 3H), 4.89−4.99 (m, 1H), 5.78 (s, 1H), 6.77−6.83 (m, 4H), 7.19 (d, J = 8.8 Hz, 1H), 7.39 (dd, J = 8.2 Hz, 1.6 Hz, 1H),7.88 (dd, J = 8.2 Hz, 1.6 Hz, 1H). ^{13}C NMR ($CDCl_3$, 150 MHz) δ: 20.27, 26.67, 37.65, 45.07, 55.94, 73.24, 101.44, 111.82, 112.09, 112.95, 116.40, 118.44, 119.35, 128.79, 129.29, 133.76, 146.75, 148.64, 155.91, 154.17, 163.64. MS (ESI, positive) m/z calcd for

DOI: 10.1021/acs.jmedchem.5b00910
J. Med. Chem. 2015, 58, 6678−6696

$C_{21}H_{21}N_2O_3$ (M + H): 349.15; found 349.30. Anal. ($C_{21}H_{20}N_2O_3$) C, H, N. HPLC purity: 97.6%.

*11-Hydroxy-15-methyl-8,9,14b,15-tetrahydrobenzofuro-[2′,3′:3,4]azepino[2,1-b]quinazolin-5(7H)-one (**54b**).* Yellow solid: 0.15 g (yield 56.2%). ^{1}H NMR (DMSO-d_6, 600 MHz) δ: 1.92−1.97 (m, 1H), 2.04−2.09 (m, 1H), 2.52−2.55 (m, 1H), 2.64−2.68 (m, 1H), 3.15−3.20 (m, 1H), 3.29 (s, 3H), 4.60−4.65 (m, 1H), 6.25 (s, 1H), 6.63 (dd, J = 8.8 Hz, 2.5 Hz, 1H), 6.72−6.75 (m, 1H), 6.76 (d, J = 2.4 Hz, 1H), 6.88 (d, J = 8.2 Hz, 1H), 7.15 (d, J = 8.8 Hz, 1H), 7.39−7.41 (m, 1H), 7.63 (dd, J = 7.7 Hz, 1.7 Hz, 1H), 9.20 (s, 1H). ^{13}C NMR (DMSO-d_6, 150 MHz) δ: 19.79, 25.93, 36.71, 44.25, 71.21, 103.42, 111.28, 112.15, 112.79, 115.67, 117.54, 118.26, 127.81, 129.22, 133.77, 146.92, 146.94, 153.31, 154.60,162.68. MS (ESI, positive) m/z calcd for $C_{20}H_{19}N_2O_3$ (M + H): 335.14; found 335.13. Anal. ($C_{20}H_{18}N_2O_3$) C, H, N. HPLC purity: 96.8%.

*7,8,13,13b-Tetrahydro-5H-benzo[5′,6′][1,3]oxazino[3′,2′:1,2]-pyrido[3,4-b]indol-5-one (**57a**).* To a solution of 2-hydroxybenzoic acid (1 g, 7.2 mmol) in DCM (50 mL), thionyl chloride (1.71 g, 14.4 mmol) was added and stirred for 1 h at 40 °C. Then, the solvent and excess thionyl chloride were removed under reduced pressure. The residue was added to a solution of intermediate **8** (1.02 g, 6 mmol) in DCM (30 mL) and stirred for 12 h at room temperature. After the reaction, the solvent was removed under reduced pressure, and the residue was purified by silica gel column chromatography (hexane/EtOAc = 4:1) to afford **57a** as a white solid (1.01 g, yield 57.6%). ^{1}H NMR (DMSO-d_6, 500 MHz) δ: 2.93−3.02 (m, 2H), 3.21−3.22 (m, 1H), 4.71−4.74 (m, 1H), 6.68 (s, 1H), 7.07 (t, J = 7.7 Hz, 1H), 7.13−7.27 (m, 3H), 7.42 (d, J = 8.2 Hz, 1H), 7.57−7.60 (m, 2H), 7.91 (d, J = 7.6 Hz, 1H), 11.52 (s, 1H). ^{13}C NMR ($CDCl_3$, 75 MHz) δ: 14.1, 39.1, 81.2, 111.6, 113.7, 116.3, 118.6, 119.3, 120.3, 123.0, 123.7, 125.9, 127.1, 128.8, 134.2, 137.2, 156.7, 163.0. MS (ESI, positive) m/z calcd for $C_{18}H_{15}N_2O_2$ (M + H): 291.32; found 291.43. Anal. ($C_{18}H_{14}N_2O_2$) C, H, N. HPLC purity: 98.6%.

*3-Chloro-10-hydroxy-7,8,13,13b-tetrahydro-5H-benzo[5′,6′][1,3]-oxazino[3′,2′:1,2]pyrido[3,4-b]indol-5-one (**58k**).* Pale solid, 0.12 g (yield 66.9%). ^{1}H NMR (DMSO-d_6, 500 MHz) δ: 2.79−2.82 (m, 2H), 3.19 (m, 1H), 4.66−4.69 (m, 1H), 6.66 (s, 1H), 6.71 (dd, J = 2.2 Hz, 8.7 Hz, 1H), 6.84 (s, 1H), 7.17−7.22 (m, 2H), 7.63 (dd, J = 2.6 Hz, 8.7 Hz, 1H), 7.83 (s, 1H), 8.78 (s, 1H), 11.18 (s, 1H). ^{13}C NMR (DMSO-d_6, 150 MHz) δ: 19.78, 40.05, 81.43, 102.57, 110.88, 112.22, 113.17, 118.72, 119.84, 125.82, 126.60, 127.12, 127.34, 131.48, 134.01, 150.76, 155.36, 161.13. MS (ESI, positive) m/z calcd for $C_{18}H_{14}ClN_2O_3$ (M + H): 341.07; found 341.90. Anal. ($C_{18}H_{13}ClN_2O_3$) C, H, N. HPLC purity: 97.0%.

*7,8,13,13b-Tetrahydro-5H-benzo[5′,6′][1,3]thiazino[3′,2′:1,2]-pyrido[3,4-b]indol-5-one (**63a**).* To a solution of 2-mercaptobenzoic acid (0.77 g, 5.0 mmol) in DCM (50 mL), thionyl chloride (1.42 g, 12 mmol) was added dropwise at room temperature. Then, the mixture was heated to 50 °C and stirred for 3 h. The solvent and excess thionyl chloride were removed under reduced pressure. The residue was added to a solution of intermediate **8** (0.51 g, 3.0 mmol) in DCM (50 mL) and stirred for 12 h at room temperature. After the reaction, the solvent was removed under reduced pressure, and the residue was purified by silica gel column chromatography (hexane/EtOAc = 4:1) to afford **63a** as a yellow solid (0.33 g, yield 36.1%). ^{1}H NMR ($CDCl_3$, 300 MHz) δ: 3.01−3.06 (m, 2H), 3.43−3.52 (m, 1H), 4.81−4.88 (m, 1H), 6.36 (s, 1H), 7.16−7.46 (m, 6H), 7.60 (d, J = 7.8 Hz, 1H), 8.21 (s, 1H), 8.23 (d, J = 1.8 Hz, 1H). ^{13}C NMR (DMSO-d_6, 150 MHz) δ: 20.60, 40.45, 56.87, 110.60, 112.11, 118.95, 119.58, 122.69, 126.08, 126.85, 127.57, 128.29, 129.47, 131.12, 132.56, 136.12, 137.31, 164.84. MS (ESI, positive) m/z calcd for $C_{18}H_{15}N_2OS$ (M + H): 307.09; found 307.50. Anal. ($C_{18}H_{14}N_2OS$) C, H, N. HPLC purity: 97.0%.

Starting from substituted *o*-aminobenzoic acid, various *o*-thiolbenzoic acids were prepared according to the method reported by Tanida's group.[52] The synthetic method for compounds **63b−63h** was similar to that of **63a**.

*3-Chloro-10-hydroxy-7,8,13,13b-tetrahydro-5H-benzo[5′,6′][1,3]-thiazino[3′,2′:1,2]pyrido[3,4-b]indol-5-one (**66c**).* Pale solid, 0.12 g (yield, 66.5%). ^{1}H NMR (DMSO-d_6, 500 MHz) δ: 2.75−2.90 (m, 2H), 3.21−3.26 (m, 1H), 4.65−4.71 (m, 1H), 6.55 (s, 1H), 6.65 (dd, J = 2.3 Hz, 8.6 Hz, 1H), 6.80 (d, J = 2.0 Hz, 1H), 7.14 (d, J = 8.6 Hz, 1H), 7.52−7.61 (m, 2H), 7.98 (d, J = 2.3 Hz, 1H), 8.79 (s, 1H), 11.02 (s, 1H). ^{13}C NMR (DMSO-d_6, 150 MHz) δ: 20.53, 40.72, 57.02, 102.84, 109.81, 112.53, 113.08, 126.74, 128.12, 129.55, 130.28, 131.04, 131.36, 131.76, 132.28, 135.25, 151.35, 163.83. MS (ESI, positive) m/z calcd for $C_{18}H_{14}ClN_2O_2S$ (M + H): 357.05; found 357.09. Anal. ($C_{18}H_{13}ClN_2O_2S$) C, H, N. HPLC purity: 95.8%.

***In Vitro* Cytotoxicity Assay.** Cells were plated in 96-well microtiter plates at a density of 5 × 10^3/well and incubated in a humidified atmosphere with 5% CO_2 at 37 °C for 24 h. Test compounds were added onto triplicate wells with different concentrations and 0.1% DMSO for the control. After they had been incubated for 72 h, 20 μL of MTT (3-(4,5-dimethylthiazol-2-yl)-2,5-diphenyltetrazolium bromide) solution (5 mg/mL) was added to each well, and the plate was incubated for an additional 4 h. The formazan was dissolved in 100 μL of DMSO. The absorbance (OD) was read on a WellscanMK-2 microplate reader (Labsystems) at 570 nm. The concentration causing 50% inhibition of cell growth (IC_{50}) was determined by the Logit method.[53] All experiments were performed three times.

Apoptosis Detection Assay. A549 cells (5 × 10^5 cells/mL) were seeded in six-well plates and treated with compounds at a concentration of 5 μM for 48 h. The cells were then harvested by trypsinization and washed twice with cold PBS. After centrifugation and removal of the supernatants, cells were resuspended in 400 μL of 1× binding buffer, which was then added to 5 μL of annexin V-FITC and incubated at room temperature for 15 min. After adding 10 μL of PI, the cells were incubated at room temperature for another 15 min in the dark. The stained cells were analyzed by a flow cytometer (BD Accuri C6).

Flow Cytometer Analysis of Cell Cycle. A549 cells (2 × 10^4 cells/mL) were treated with various concentrations of compounds **58k** or **66a** for 0−36 h. The treated cells were collected, resuspended, and incubated for 30 min at 37 °C with 25 μg/mL PI and 10 μg/mL RNase buffer. For each sample, at least 1 × 10^4 cells were analyzed using flow cytometry (BD Accuri C6).

Top1 Inhibitory Activity Assay. The Top1 inhibition assay was performed according to the procedure described in our previous studies.[33,34] Briefly, the assay mixture contained 35 mM Tris-HCl (pH 8.0), 72 mM KCl, 5 mM $MgCl_2$, 5 mM dithiothreitol, 5 mM spermidine, 0.1% bovine serum albumin (BSA), pBR322 plasmid DNA (0.25 μg), the indicated drug concentrations (1% DMSO), and 1 unit of Top1 (TaKaRa Biotechnology Co., Ltd., Dalian) in a final volume of 20 μL. Assay mixtures were incubated for 15 min at 37 °C and stopped by the addition of 2 μL of 10× loading buffer (0.9% sodium dodecyl sulfate (SDS), 0.05% bromophenol blue, and 50% glycerol). Electrophoresis was carried out in a 0.8% agarose gel in TAE (Tris-acetate-EDTA) at 8 V/cm for 1 h. Gels were stained with ethidium bromide (0.5 μg/mL) for 60 min, and the DNA band was visualized over UV light and photographed with a Gel Doc Ez imager (Bio-Rad Laboratories Ltd.).

Top2 Inhibitory Activity Assay. The DNA Top2α inhibition assay was performed according to our previous study.[34] Briefly, the assay mixture contained 50 mM Tris-HCl (pH 8.0), 150 mM NaCl, 10 mM $MgCl_2$, 5 mM dithiothreitol, 30 μg/mL bovine serum albumin (BSA), 2 mM ATP, pBR322 plasmid DNA (0.25), the indicated drug concentrations (1% DMSO), and 0.75 unit of Top2α (TopoGEN, Inc.) in a final volume of 20 μL. Reaction mixtures were incubated for 30 min at 37 °C and stopped by the addition of 2 μL of 10% SDS. Then, 2 μL of 10× gel loading buffer (0.25% bromophenol blue and 50% glycerol) was added. Electrophoresis was carried out in a 1% agarose gel in TAE (Tris-acetate-EDTA) at 8 V/cm for 1 h. Gels were stained with ethidium bromide (0.5 μg/mL) for 60 min, and the DNA band was visualized over UV light and photographed with a Gel Doc Ez imager (Bio-Rad Laboratories Ltd.).

Tubulin Polymerization Inhibitory Activity Assay. A tubulin polymerization assay was performed according to the literature.[54] Purified brain tubulin polymerization kit was purchased from Cytoskeleton (BK006P, Denver, CO). The final assay buffer containing 0.1 M MES (pH 6.6), 10 mM $MgCl_2$, 1 mM GTP, 1 mM EGTA, and 3.4 M glycerol was cooled to 0 °C. Compounds **58k** and **66c** were added in different concentrations, and then, the reaction was initiated by the addition of tubulin to a final concentration of 10 mM and warmed to 37

DOI: 10.1021/acs.jmedchem.5b00910
J. Med. Chem. 2015, 58, 6678−6696

°C. Colchicine and vinorelbine were used as positive controls under similar experimental conditions (Figure S1). The optical density at 340 nm was measured for 15−30 at 1 min intervals in BioTek's Synergy 4 multifunction microplate reader. Assays were performed twice, and the average data were used for calculating IC_{50} values and plotting figures.

Molecular Modeling. Selected compounds were docked into the active site of Top1 or Top2α by a procedure similar to that described previously.[33,34] For docking tubulin inhibitors, the X-ray crystallographic structure 1SA0 was used. A Glide 5.9 module in Maestro 9.4 software with extra precision setting was used for docking simulations. First, we docked colchicine into tubulin to check the reliability of the docking method. Glide 5.9 with extra precision setting successfully reproduced the experimental poses as the best ranked solutions with a ligand RMSD value of 0.90 Å. Molecular dynamics simulations were performed to validate the binding poses obtained by molecular docking. Desmond (version Desmond_Maestro_academic-2009-02) was used to carry out the dynamic simulations, and the detailed parameters were similar to those in our previous studies.[33,34] The results indicated that the docked pose and stable conformation after MD calculations were similar, with RMSD values lower than 2 Å, and that important hydrogen bonding interactions were retained.

***In Vivo* Antitumor Activity.** Compounds **58g**, **58i**, **58k**, **66a**, **66c**, and **66e** at the dose of 2 mg/kg were selected for evaluating *in vivo* antitumor activity. TPT at 0.5 mg/kg was used as the control. BALB/C nude male mice (certificate SCXK-2007-0005, weighing 18−20 g) were obtained from the Shanghai Experimental Animal Center, Chinese Academy of Sciences. A549 lung cancer cell suspensions or HCT116 colon cancer cell suspensions were implanted subcutaneously into the right axilla region of the mice. Treatment began when implanted tumors had reached a volume of about 100−300 mm^3 (after 17 days). The animals were randomized into appropriate groups (6 animals/treatment and 10 animals/control group) and administered by ip injection for five consecutive days once on day 17 after the implantation of cells. Observation was conducted after the first dosing and lasted over 15 days. Tumor volumes were monitored by caliper measurements of the length and width and calculated using the formula of $TV = {}^1/_2 \times a \times b^2$, where a is the tumor length, and b is the width. Tumor volumes and body weights were monitored every 4 days over the course of treatment. Mice were sacrificed on day 30−33 after the implantation of cells, and tumors were removed and recorded for analysis.

■ ASSOCIATED CONTENT

Supporting Information

The Supporting Information is available free of charge on the ACS Publications website at DOI: 10.1021/acs.jmedchem.5b00910.

Experimental protocols and structural characterization of target compounds; biological assays and the inhibition rate of compounds **58k** and **66c** against a panel of 31 antitumor targets; the effects of several target compounds on Top1, Top2, tubulin, and cell cycle distribution; the change of body weight for the nude mice treated with selected derivatives
(PDF)

■ AUTHOR INFORMATION

Corresponding Author

*Phone: 86-21-81871239. E-mail: shengcq@hotmail.com.

Author Contributions

‖S.W., K.F., and G.D. contributed equally to this work.

Notes

The authors declare no competing financial interest.

■ ACKNOWLEDGMENTS

This work was supported in part by the National Natural Science Foundation of China (Grants 81373278 and 8122044), the 863 Hi-Tech Program of China (grant 2014AA020525), Science and Technology Commission of Shanghai (grant 11431920402 and 14YF1405400), and Shanghai "ShuGuang" Project (grant 14SG33).

■ ABBREVIATIONS USED

NP, natural product; Top1, topoisomerase I; Top2, topoisomerase II; CPT, camptothecin; TPT, topotecan; IRT, irinotecan; SAR, structure−activity relationship; BIOS, biology-oriented synthesis; DOS, diversity-oriented synthesis; DTS, diverted total synthesis

■ REFERENCES

(1) Newman, D. J.; Cragg, G. M. Natural products as sources of new drugs over the 30 years from 1981 to 2010. *J. Nat. Prod.* **2012**, *75*, 311−335.

(2) Newman, D. J.; Cragg, G. M. Natural products as sources of new drugs over the last 25 years. *J. Nat. Prod.* **2007**, *70*, 461−477.

(3) Newman, D. J.; Cragg, G. M.; Snader, K. M. Natural products as sources of new drugs over the period 1981−2002. *J. Nat. Prod.* **2003**, *66*, 1022−1037.

(4) Wetzel, S.; Bon, R. S.; Kumar, K.; Waldmann, H. Biology-oriented synthesis. *Angew. Chem., Int. Ed.* **2011**, *50*, 10800−10826.

(5) Bon, R. S.; Waldmann, H. Bioactivity-guided navigation of chemical space. *Acc. Chem. Res.* **2010**, *43*, 1103−1114.

(6) Kaiser, M.; Wetzel, S.; Kumar, K.; Waldmann, H. Biology-inspired synthesis of compound libraries. *Cell. Mol. Life Sci.* **2008**, *65*, 1186−1201.

(7) Dandapani, S.; Marcaurelle, L. A. Current strategies for diversity-oriented synthesis. *Curr. Opin. Chem. Biol.* **2010**, *14*, 362−370.

(8) Cordier, C.; Morton, D.; Murrison, S.; Nelson, A.; O'Leary-Steele, C. Natural products as an inspiration in the diversity-oriented synthesis of bioactive compound libraries. *Nat. Prod. Rep.* **2008**, *25*, 719−737.

(9) Wilson, R. M.; Danishefsky, S. J. Small molecule natural products in the discovery of therapeutic agents: the synthesis connection. *J. Org. Chem.* **2006**, *71*, 8329−8351.

(10) Njardarson, J. T.; Gaul, C.; Shan, D.; Huang, X. Y.; Danishefsky, S. J. Discovery of potent cell migration inhibitors through total synthesis: lessons from structure-activity studies of (+)-migrastatin. *J. Am. Chem. Soc.* **2004**, *126*, 1038−1040.

(11) Danishefsky, S. On the potential of natural products in the discovery of pharma leads: a case for reassessment. *Nat. Prod. Rep.* **2010**, *27*, 1114−1116.

(12) Grabowski, K.; Baringhaus, K. H.; Schneider, G. Scaffold diversity of natural products: inspiration for combinatorial library design. *Nat. Prod. Rep.* **2008**, *25*, 892−904.

(13) O'Connor, C. J.; Beckmann, H. S.; Spring, D. R. Diversity-oriented synthesis: producing chemical tools for dissecting biology. *Chem. Soc. Rev.* **2012**, *41*, 4444−4456.

(14) Antonchick, A. P.; Gerding-Reimers, C.; Catarinella, M.; Schurmann, M.; Preut, H.; Ziegler, S.; Rauh, D.; Waldmann, H. Highly enantioselective synthesis and cellular evaluation of spirooxindoles inspired by natural products. *Nat. Chem.* **2010**, *2*, 735−740.

(15) Chiou, W. F.; Sung, Y. J.; Liao, J. F.; Shum, A. Y.; Chen, C. F. Inhibitory effect of dehydroevodiamine and evodiamine on nitric oxide production in cultured murine macrophages. *J. Nat. Prod.* **1997**, *60*, 708−711.

(16) Ko, H. C.; Wang, Y. H.; Liou, K. T.; Chen, C. M.; Chen, C. H.; Wang, W. Y.; Chang, S.; Hou, Y. C.; Chen, K. T.; Chen, C. F.; Shen, Y. C. Anti-inflammatory effects and mechanisms of the ethanol extract of Evodia rutaecarpa and its bioactive components on neutrophils and microglial cells. *Eur. J. Pharmacol.* **2007**, *555*, 211−217.

(17) Liu, Y. N.; Pan, S. L.; Liao, C. H.; Huang, D. Y.; Guh, J. H.; Peng, C. Y.; Chang, Y. L.; Teng, C. M. Evodiamine represses hypoxia-induced inflammatory proteins expression and hypoxia-inducible factor 1alpha accumulation in RAW264.7. *Shock* **2009**, *32*, 263−269.

DOI: 10.1021/acs.jmedchem.5b00910
J. Med. Chem. 2015, 58, 6678−6696

(18) Kobayashi, Y.; Nakano, Y.; Kizaki, M.; Hoshikuma, K.; Yokoo, Y.; Kamiya, T. Capsaicin-like anti-obese activities of evodiamine from fruits of Evodia rutaecarpa, a vanilloid receptor agonist. *Planta Med.* **2001**, *67*, 628−633.
(19) Bak, E. J.; Park, H. G.; Kim, J. M.; Yoo, Y. J.; Cha, J. H. Inhibitory effect of evodiamine alone and in combination with rosiglitazone on in vitro adipocyte differentiation and in vivo obesity related to diabetes. *Int. J. Obes.* **2010**, *34*, 250−260.
(20) Wang, T.; Wang, Y.; Kontani, Y.; Kobayashi, Y.; Sato, Y.; Mori, N.; Yamashita, H. Evodiamine improves diet-induced obesity in a uncoupling protein-1-independent manner: involvement of antiadipogenic mechanism and extracellularly regulated kinase/mitogen-activated protein kinase signaling. *Endocrinology* **2008**, *149*, 358−366.
(21) Wang, T.; Wang, Y.; Yamashita, H. Evodiamine inhibits adipogenesis via the EGFR-PKCalpha-ERK signaling pathway. *FEBS Lett.* **2009**, *583*, 3655−3659.
(22) Jiang, J.; Hu, C. Evodiamine: a novel anti-cancer alkaloid from Evodia rutaecarpa. *Molecules* **2009**, *14*, 1852−1859.
(23) Yu, H.; Jin, H.; Gong, W.; Wang, Z.; Liang, H. Pharmacological actions of multi-target-directed evodiamine. *Molecules* **2013**, *18*, 1826−1843.
(24) Kan, S. F.; Yu, C. H.; Pu, H. F.; Hsu, J. M.; Chen, M. J.; Wang, P. S. Anti-proliferative effects of evodiamine on human prostate cancer cell lines DU145 and PC3. *J. Cell. Biochem.* **2007**, *101*, 44−56.
(25) Chen, M. C.; Yu, C. H.; Wang, S. W.; Pu, H. F.; Kan, S. F.; Lin, L. C.; Chi, C. W.; Ho, L. L.; Lee, C. H.; Wang, P. S. Anti-proliferative effects of evodiamine on human thyroid cancer cell line ARO. *J. Cell. Biochem.* **2010**, *110*, 1495−1503.
(26) Zhang, C.; Fan, X.; Xu, X.; Yang, X.; Wang, X.; Liang, H. P. Evodiamine induces caspase-dependent apoptosis and S phase arrest in human colon lovo cells. *Anti-Cancer Drugs* **2010**, *21*, 766−776.
(27) Wang, K. L.; Hsia, S. M.; Yeh, J. Y.; Cheng, S. C.; Wang, P. S.; Wang, S. W. Anti-Proliferative Effects of Evodiamine on Human Breast Cancer Cells. *PLoS One* **2013**, *8*, e67297.
(28) Yang, L.; Liu, X.; Wu, D.; Zhang, M.; Ran, G.; Bi, Y.; Huang, H. Growth inhibition and induction of apoptosis in SGC7901 human gastric cancer cells by evodiamine. *Mol. Med. Rep.* **2014**, *9*, 1147−1152.
(29) Lee, T. J.; Kim, E. J.; Kim, S.; Jung, E. M.; Park, J. W.; Jeong, S. H.; Park, S. E.; Yoo, Y. H.; Kwon, T. K. Caspase-dependent and caspase-independent apoptosis induced by evodiamine in human leukemic U937 cells. *Mol. Cancer Ther.* **2006**, *5*, 2398−2407.
(30) Huang, H.; Zhang, Y.; Liu, X.; Li, Z.; Xu, W.; He, S.; Huang, Y.; Zhang, H. Acid sphingomyelinase contributes to evodiamine-induced apoptosis in human gastric cancer SGC-7901 cells. *DNA Cell Biol.* **2011**, *30*, 407−412.
(31) Liu, A. J.; Wang, S. H.; Chen, K. C.; Kuei, H. P.; Shih, Y. L.; Hou, S. Y.; Chiu, W. T.; Hsiao, S. H.; Shih, C. M. Evodiamine, a plant alkaloid, induces calcium/JNK-mediated autophagy and calcium/mitochondria-mediated apoptosis in human glioblastoma cells. *Chem.-Biol. Interact.* **2013**, *205*, 20−28.
(32) Wang, C.; Li, S.; Wang, M. W. Evodiamine-induced human melanoma A375-S2 cell death was mediated by PI3K/Akt/caspase and Fas-L/NF-kappaB signaling pathways and augmented by ubiquitin-proteasome inhibition. *Toxicol. In Vitro* **2010**, *24*, 898−904.
(33) Dong, G.; Sheng, C.; Wang, S.; Miao, Z.; Yao, J.; Zhang, W. Selection of evodiamine as a novel topoisomerase I inhibitor by structure-based virtual screening and hit optimization of evodiamine derivatives as antitumor agents. *J. Med. Chem.* **2010**, *53*, 7521−7531.
(34) Dong, G.; Wang, S.; Miao, Z.; Yao, J.; Zhang, Y.; Guo, Z.; Zhang, W.; Sheng, C. New tricks for an old natural product: discovery of highly potent evodiamine derivatives as novel antitumor agents by systemic structure-activity relationship analysis and biological evaluations. *J. Med. Chem.* **2012**, *55*, 7593−7613.
(35) Li, Z.; Dong, G.; Wang, S.; Miao, Z.; Yao, J.; Zhang, W.; Sheng, C. Optical evodiamine derivatives: asymmetric synthesis and antitumor activity. *Chin. Chem. Lett.* **2015**, *26*, 267−271.
(36) Fang, K.; Dong, G.; Gong, H.; Liu, N.; Li, Z.; Zhu, S.; Miao, Z.; Yao, J.; Zhang, W.; Sheng, C. Design, synthesis and biological evaluation of E-ring modified evodiamine derivatives as novel antitumor agents. *Chin. Chem. Lett.* **2014**, *25*, 978−982.
(37) Ivanova, B.; Spiteller, M. Evodiamine and rutaecarpine alkaloids as highly selective transient receptor potential vanilloid 1 agonists. *Int. J. Biol. Macromol.* **2014**, *65*, 314−324.
(38) Christodoulou, M. S.; Sacchetti, A.; Ronchetti, V.; Caufin, S.; Silvani, A.; Lesma, G.; Fontana, G.; Minicone, F.; Riva, B.; Ventura, M.; Lahtela-Kakkonen, M.; Jarho, E.; Zuco, V.; Zunino, F.; Martinet, N.; Dapiaggi, F.; Pieraccini, S.; Sironi, M.; Dalla Via, L.; Gia, O. M.; Passarella, D. Quinazolinecarboline alkaloid evodiamine as scaffold for targeting topoisomerase I and sirtuins. *Bioorg. Med. Chem.* **2013**, *21*, 6920−6928.
(39) Song, S.; Chen, Z.; Li, S.; Huang, Y.; Wan, Y.; Song, H. Design, synthesis and evaluation of N13-substituted evodiamine derivatives against human cancer cell lines. *Molecules* **2013**, *18*, 15750−15768.
(40) Barker, J. M.; Huddleston, P. R.; Wood, M. L. A rapid conversion of 3-oxothiolanes into 3-aminothiophenes. *Synth. Commun.* **2002**, *32*, 2565−2568.
(41) Sircar, J.; Kumar, K. C. S.; Davis, T. J.; Ying, W. Preparation of 4-Acylpiperazin-1-yl-Substituted Thienopyridinone Derivatives as Macrophage Migration Inhibitory Factor Inhibitors. WO2006102191A1, 2006.
(42) Yin, Q.; Wang, S. G.; You, S. L. Asymmetric synthesis of tetrahydro-beta-carbolines via chiral phosphoric acid catalyzed transfer hydrogenation reaction. *Org. Lett.* **2013**, *15*, 2688−2691.
(43) Wipf, P.; Wang, Q. J. Preparation of Benzothienothiazepinone Derivatives and Analogs for Use as Protein Kinase D Inhibitors. WO2012078859A2, 2012.
(44) Kajino, M.; Imaeda, T. Preparation of 1,3-Benzothiazinone Derivatives Having a Capability of Binding to a Macrophage Migration Inhibitory Factor (MIF) and Activating of an Antioxidant Response Element (ARE). WO2006132438A1, 2006.
(45) Huang, D. M.; Guh, J. H.; Huang, Y. T.; Chueh, S. C.; Chiang, P. C.; Teng, C. M. Induction of mitotic arrest and apoptosis in human prostate cancer pc-3 cells by evodiamine. *J. Urol.* **2005**, *173*, 256−261.
(46) Rudolf, E.; Cervinka, M. Topoisomerases and tubulin inhibitors: a promising combination for cancer treatment. *Curr. Med. Chem.: Anti-Cancer Agents* **2003**, *3*, 421−429.
(47) Diana, P.; Martorana, A.; Barraja, P.; Montalbano, A.; Dattolo, G.; Cirrincione, G.; Dall'acqua, F.; Salvador, A.; Vedaldi, D.; Basso, G.; Viola, G. Isoindolo[2,1-a]quinoxaline derivatives, novel potent antitumor agents with dual inhibition of tubulin polymerization and topoisomerase I. *J. Med. Chem.* **2008**, *51*, 2387−2399.
(48) Yi, J. M.; Zhang, X. F.; Huan, X. J.; Song, S. S.; Wang, W.; Tian, Q. T.; Sun, Y. M.; Chen, Y.; Ding, J.; Wang, Y. Q.; Yang, C. H.; Miao, Z. H. Dual targeting of microtubule and topoisomerase II by alpha-carboline derivative YCH337 for tumor proliferation and growth inhibition. *Oncotarget* **2015**, *6*, 8960−8973.
(49) Liu, J.; Zheng, C. H.; Ren, X. H.; Zhou, F.; Li, W.; Zhu, J.; Lv, J. G.; Zhou, Y. J. Synthesis and biological evaluation of 1-benzylidene-3,4-dihydronaphthalen-2-one as a new class of microtubule-targeting agents. *J. Med. Chem.* **2012**, *55*, 5720−5733.
(50) Reddy, P. A. P.; Wong, T. T.; Zhao, L.; Tang, S.; Labroli, M. A.; Guzi, T. J.; Siddiqui, M. A. Preparation of Thiazole Derivatives as Protein Kinase Inhibitors. WO2009058728A1, 2009.
(51) Lyubchanskaya, V. M.; Alekseeva, L. M.; Savina, S. A.; Shashkov, A. S.; Granik, V. G. α-Oxolactam enamines as new synthons in the Nenitzescu reaction. *Russ. Chem. Bull.* **2002**, *51*, 1886−1893.
(52) Kimura, H.; Sato, Y.; Tajima, Y.; Suzuki, H.; Yukitake, H.; Imaeda, T.; Kajino, M.; Oki, H.; Takizawa, M.; Tanida, S. BTZO-1, a cardioprotective agent, reveals that macrophage migration inhibitory factor regulates ARE-mediated gene expression. *Chem. Biol.* **2010**, *17*, 1282−1294.
(53) Huang, H.; Chen, Q.; Ku, X.; Meng, L.; Lin, L.; Wang, X.; Zhu, C.; Wang, Y.; Chen, Z.; Li, M.; Jiang, H.; Chen, K.; Ding, J.; Liu, H. A series of alpha-heterocyclic carboxaldehyde thiosemicarbazones inhibit topoisomerase IIalpha catalytic activity. *J. Med. Chem.* **2010**, *53*, 3048−3064.

DOI: 10.1021/acs.jmedchem.5b00910
J. Med. Chem. 2015, 58, 6678−6696

(54) Shelanski, M. L.; Gaskin, F.; Cantor, C. R. Microtubule assembly in the absence of added nucleotides. *Proc. Natl. Acad. Sci. U. S. A.* **1973**, *70*, 765−768.

DOI: 10.1021/acs.jmedchem.5b00910
J. Med. Chem. 2015, 58, 6678−6696